Hydrol. Earth Syst. Sci. Discuss., 11, 10593–10633, 2014
www.hydrol-earth-syst-sci-discuss.net/11/10593/2014/
doi:10.5194/hessd-11-10593-2014

Hydrology and Earth System Sciences
Open Access
Discussions

Reconciling the dynamic relationship between climate variables and vegetation productivity into a hydrological model to improve streamflow prediction under climate change

Z. K. Tesemma, Y. Wei, M. C. Peel, and A. W. Western

Department of Infrastructure Engineering, The University of Melbourne, Parkville, 3010, Victoria, Australia

Received: 25 August 2014 – Accepted: 1 September 2014 – Published: 23 September 2014

Correspondence to: Y. Wei (ywei@unimelb.edu.au)

Published by Copernicus Publications on behalf of the European Geosciences Union.

Abstract

Anthropogenic climate change is projected to enrich the atmosphere with carbon dioxide, change vegetation dynamics and influence the availability of water at the catchment. This study combines a simple model for estimating changes in leaf area index (LAI) due to climate fluctuations with the variable infiltration capacity (VIC) land surface model to improve catchment streamflow prediction under a changing climate. The combined model was applied to thirteen gauged catchments with different land cover types (crop, pasture and tree) in the Goulburn–Broken catchment, Australia during the "Millennium Drought" (2000–2009), and two future periods (2021–2050 and 2071–2100) for two emission scenarios (RCP4.5 and RCP8.5). The future climatic and modelled streamflow results were compared with the baseline historical period of 1981–2010. This region is projected to be warmer and mostly drier in the future as predicted by 38 Coupled Model Inter-comparison Project Phase 5 (CMIP5) simulations from 15 Global Climate Models (GCMs) and for two emission scenarios. The results showed that during the Millennium Drought there was about a 30–65 % reduction in mean annual runoff due to reduced rainfall and increased temperature. This climate based reduction in mean annual runoff was partially offset by a drought related decline in LAI that reduced the climate related reduction of mean annual runoff, effectively increased runoff, by 2–9 %. Projected climate change may reduce mean annual runoff by between 6 and 31 % in the study catchments. However, when LAI is allowed to respond to changes in climate the projected declines in runoff were reduced to between 2 and 22 % in comparison to when the historical LAI was considered. Incorporating changes in LAI in VIC to respond to changing climate reduced the projected declines in streamflow and confirms the importance of including the effects of changes in vegetation productivity in future projections of streamflow.

HESSD
11, 10593–10633, 2014

1 Introduction

Recent climate changes have been observed in different parts of Australia (Chiew et al., 2011; Cai and Cowan, 2008; Hughes et al., 2012; Lockart et al., 2009; Potter and Chiew, 2011). Specifically, south-eastern Australian catchments have experienced changes in streamflow due to fluctuations in climate as observed during the recent "Millennium Drought" (1997–2009) which lasted more than a decade (Chiew et al., 2011; Verdon-Kidd and Kiem, 2009). This drought may be representative of future climatic conditions.

The projected water availability for future climates derived from downscaled outputs from global and regional climate models indicate increases of mean annual runoff by 10 to 40 % in some parts of the world (high northern latitudes) and 10 to 30 % reduction elsewhere (southern Europe, Middle East and south-eastern Australia) (Milly et al., 2005). More recently, Roderick and Farquhar (2011) examined climate and catchment characteristics for sensitivity to changes in runoff from a theoretical point of view and estimated that a 10 % change in rainfall would lead to a 26 % change in runoff and a 10 % change in potential evaporation would lead to a 16 % change in runoff with all other variables being constant. In south-eastern Australia it has been projected that there will be a reduction in mean annual runoff of 10 % on average when different climate models are used as input to hydrological models (Cai and Cowan, 2008; Chiew et al., 2009; Roderick and Farquhar, 2011; Teng et al., 2012a; Vaze and Teng, 2011). These studies assessed the possible impacts of climate change on total runoff based only on rainfall–runoff relationships which considered first order effects of changes in precipitation and temperature with subsequent impacts on evaporative demand. However, there is evidence that such relationships are not stationary over time (Chiew et al., 2014; Peel and Blöschl, 2011; Vaze et al., 2010). One approach to improving modelling under changing conditions is to use variable monthly leaf area index (LAI) to drive the hydrologic model, which has been shown to improve model performance relative to driving the model with mean monthly LAI under wet and dry

HESSD
11, 10593–10633, 2014

climatic conditions (Tesemma et al., 2014b). LAI primarily responds to the availability of water and changes in vegetation type, such as conversion of forest to cropland or pasture, but also responds, to a less extent, to changes in temperature and rising atmospheric CO_2 concentrations. Most of these LAI responses are expected to be affected by projected climate change. Climate-induced changes in vegetation may impact on evapotranspiration and runoff through changes in vegetation productivity and changes in soil moisture which, in turn, affect runoff generation. The Dynamic global vegetation models (DGVMs) has been used to assess the vegetation effect of climate change on large-scale water balance (Murray et al., 2012, 2011). However most DGVMs overestimate runoff mainly due to model structure problem along operating at low spatial and temporal resolution (Murray et al., 2013). Thus the indirect effect of changes in precipitation and temperature as inputs into vegetation productivity on hydrological response at catchment scale has been rarely studied. The relationships between vegetation productivity or LAI and climate fluctuation has been modelled (Ellis and Hatton, 2008; O'Grady et al., 2011; Jahan and Gan, 2011; Palmer et al., 2010; Tesemma et al., 2014a; White et al., 2010), but none of them have been reconciled into hydrological models for assessing future climate change impacts on streamflow. This limits understanding of the linkages between climate fluctuations and vegetation dynamics, and their impacts and feedback on hydrological processes.

The main objective of this study is to take account of the dynamic interaction between vegetation productivity and climatic fluctuations in a hydrological model to assess their impacts on catchment runoff under projected climate change. The approach taken is to reconcile a nonlinear model that relates LAI to climate fluctuations (Tesemma et al., 2014a) into the variable infiltration capacity (VIC) hydrological model, which is forced with both historical and future downscaled Global Climate Models (GCMs) outputs. The results are discussed in the context of observed historical and projected future climatic conditions.

HESSD
11, 10593–10633, 2014

2 Research approach

This section provides details about the characteristics of the selected catchments and the modelling exercises: first, the climate and land cover of the study catchments are briefly described in Sect. 2.1; second, the modelling approach used to assess the impact of changes in climate on runoff (Sect. 2.2).

2.1 Characteristics of selected catchments

All the study catchments are located in the Goulburn–Broken catchment which is a tributary of the Murray–Darling Basin (MDB). The Goulburn–Broken catchment extends between 35.8 to 37.7° S and between 144.6 to 146.7° E (Fig. 1a) with a range of altitude from approximately 1790 m on the southern side to 86 m above mean sea level (a.m.s.l.) on the northern side of the catchment. The selected catchments mean annual rainfall range from 659 to 1407 mm year^{-1} calculated for the period (1982–2012). The majority of the rainfall (about 60 %) occurs during winter and spring. Following the spatial variation in mean annual temperature, the reference evapotranspiration (PET), using the Food and Agricultural Organization (FAO56) method, ranges from 903 to 1046 mm year^{-1}. Hence, the dryness index (mean annual reference evapotranspiration divided by mean annual precipitation) varies from 0.64 to 1.6 (Fig. 1b). The dominant land cover type in most of the catchment is forest (mainly open Eucalyptus tall trees and Eucalyptus woodlands) with some pasture in all catchments. Limited cropland is located in some of the catchments (Fig. 1c).

2.2 Modelling research approach

The study used a rigorously calibrated and validated VIC model over the selected catchments in the Goulburn–Broken region. First the calibrated model was forced with inputs of historical climate data and LAI data modelled from historical climate data, to establish baseline streamflow estimates. Then the model was forced with projected

HESSD
11, 10593–10633, 2014

future climate inputs and corresponding modelled LAI to produce projected streamflow for future scenarios. Finally the future climates were input with the historical LAI data as used in the first simulation to produce estimates of streamflow. The detailed modelling approach of this study is described in three steps below.

2.2.1 Applying multiple GCMs and multiple emission scenarios

Outputs from many climate models from the Coupled Model Inter-comparison Project Phase 5 (CMIP5) (Taylor et al., 2012) are used as input to the hydrological model. CMIP5 contains model runs for four representative concentration pathways (RCPs), which provide radiative forcing scenarios over the 21st century (Moss et al., 2010; Vuuren et al., 2011). In this study two emission scenarios were chosen: a midrange mitigation scenario, referred to as RCP4.5 and a high emissions scenario RCP8.5 (Meinshausen et al., 2011). RCP4.5 results in a radiative forcing value of 4.5 $W m^{-2}$ at the end of the 21st century relative to the preindustrial value. While RCP8.5 provides a radiative forcing increases throughout the 21st century to a maximum of 8.5 $W m^{-2}$ at the end of the century.

CMIP5 Global Climate Model (GCM) data were collected from http://climexp.knmi.nl (accessed 28 February 2014). These data were re-sampled to a common grid resolution of 2.50° since each GCM has a different spatial resolution (some are the same, but most are different). A total of 38 RCP4.5 and RCP8.5 runs from 15 different GCM models have been used in this study. For each of the 38 runs daily precipitation, minimum and maximum temperature data were collected for three periods, 1981–2010 (in a historical run), 2021–2050 and 2071–2100 (in a future run). The study area is covered by four GCM grid cells so the areal weighted average precipitation, minimum and maximum temperature were computed. Then the areal weighted values were statistically downscaled using the delta change method. One of the advantages of using this method is that an observed database is used as the baseline resulting in a consistent set of scenario data. The delta values are estimated as follows:

HESSD
11, 10593–10633, 2014

$$\Delta_T(j) = \overline{T}_{projn}(j) - \overline{T}_{baseline}(j) \quad (1)$$

$$T_\Delta(j,i) = T_{obs}(j,i) + \Delta_T(j) \quad (2)$$

where Δ_T (j) is the delta change in 30 year mean monthly minimum or maximum temperature as simulated by the climate model $\overline{T}_{projn}(j)$ for two future periods (2021–2050 and 2071–2100) relative to the baseline period (1981–2010) climate model simulation $\overline{T}_{baseline}(j)$; $T_\Delta(j,i)$ is a statistically downscaled minimum or maximum daily temperature for the projected future climate change scenario for month j and day i; $T_{obs}(j,i)$ is observed minimum or maximum daily temperature for the historical period (1981–2010) for month j and day i. In a similar way the delta change in precipitation can also be described by the following equations:

$$\Delta_P(j) = \frac{\overline{P}_{projn}(j)}{\overline{P}_{baseline}(j)} \quad (3)$$

$$P_\Delta(j,i) = P_{obs}(j,i) \times \Delta_P(j) \quad (4)$$

where Δ_P (j) is the delta change in 30 year mean monthly precipitation as simulated by the climate model $\overline{P}_{projn}(j)$ for two future periods (2021–2050 and 2071–2100) relative to the baseline simulation $\overline{P}_{baseline}(j)$; $P_\Delta(j,i)$ is the statistically downscaled daily precipitation for the projected future climate change scenario for month j and day i, $P_{obs}(j,i)$ is observed daily precipitation for the historical period (1981–2010) for month j and day i.

2.2.2 Developed relationship between LAI and climate variables

Tesemma et al. (2014a) showed that monthly LAI of each of the vegetation types were closely related with changes in moisture state (precipitation minus reference

HESSD
11, 10593–10633, 2014

evapotranspiration) of six-monthly moving averages for crop and pasture, and nine-monthly moving averages for trees. The differences in response for the same change in moisture state among the three vegetation types were also observed in the differences in the model parameters. Tesemma et al. (2014a) provides details on the derivation of the LAI–Climate relationship for the Goulburn–Broken catchment.

$$\mathrm{LAI} = \begin{cases} \dfrac{136.4836}{1+\exp\left(-\left(\frac{(P-\mathrm{PET})-159.4555}{42.5607}\right)\right)}, & \text{if Crop} \\ \dfrac{6.2495}{1+\exp\left(-\left(\frac{(P-\mathrm{PET})-43.6157}{62.8487}\right)\right)}, & \text{if Pasture} \\ \dfrac{4.2091}{1+\exp\left(-\left(\frac{(P-\mathrm{PET})+57.1849}{36.9481}\right)\right)}, & \text{if Tree} \end{cases} \quad (5)$$

where LAI is the leaf area index of the cover type (tree/pasture/crop), P is the six month moving average for precipitation of crop and pasture, and the nine month moving average for trees, and PET is the respective reference evapotranspiration.

The monthly LAI was then simulated for both historical and future climate scenarios using the LAI–Climate model (Eq. 5) which is given by driving with the required climate inputs. The reference evapotranspiration (PET) for future climate scenarios was computed using the projected minimum and maximum temperatures keeping the other inputs of wind speed, actual vapour pressure, and solar radiation the same as the historical observations during 1981–2010. The precipitation was used for historical or future projected climate accordingly. The potential LAI variations in the baseline years (1981–2010) and the two future periods (2021–2050 and 2071–2100) and for each of the two future emission scenarios were simulated using the outputs from the 38 CMIP5 runs of the 15 GCMs into the LAI model (Eq. 5). The uncertainty ranges in modelled LAI were determined from using the different GCM runs individually into the LAI–Climate model and comparison with the mean monthly LAI in the baseline years.

HESSD
11, 10593–10633, 2014

2.2.3 Hydrological model and experimental design

In this study we used the three layer variable infiltration capacity model (VIC) model which has been used in different parts of the world and found to successfully simulate water balance components. The ability of the model to incorporate spatial representation of climate and inputs of soil, vegetation and other landscape properties make it applicable for climate and land use/land cover change impact studies. The calibrated and validated VIC model used in this study was described by Tesemma et al. (2014b).

Two model experiments were run: the first experiment considered the recent historical climate (Millennium Drought, 1997–2009) and LAI estimates using the simple LAI–Climate model against the relatively normal historical climate period (1983–1995). The second experiment considered the future climate from 38 CMIP5 runs and corresponding LAI derivatives for two periods (2021–2050 and 2071–2100), and two emission scenarios RCP4.5 and RCP8.5 with respect to the historical period (1981–2010). From the simulated flows using the above experiments changes and proportion in flow were determined: (1) the climate change effect (CC effect) which is the effect of change in precipitation and temperature due to climate change (Eq. 6), (2) the net climate change effect (CC + LAI effect) which is the effect of change in precipitation and temperature as a primary input into the model plus vegetation productivity effect of change in precipitation and temperature (Eq. 7); and (3) the proportion of CC effect on streamflow which is offset by change in LAI due to climate change (Eq. 8). Both simulations were performed over the selected thirteen calibrated sub-catchments in the Goulburn–Broken (Fig. 1b) and the flow chart of the modelling method is given on (Fig. 2).

$$Q_{\text{clim}} = \left[\frac{100 \cdot \left(Q^{\text{future climate}}_{\text{historical LAI}} - Q^{\text{historical climate}}_{\text{historical LAI}} \right)}{Q^{\text{historical climate}}_{\text{historicalLAI}}} \right] \quad (6)$$

HESSD
11, 10593–10633, 2014

$$Q_{\text{net}} = \left[\frac{100 \cdot \left(Q^{\text{future climate}}_{\text{future LAI}} - Q^{\text{historical climate}}_{\text{historical LAI}} \right)}{Q^{\text{historical climate}}_{\text{historical LAI}}} \right] \quad (7)$$

$$Q_{\text{lai}} = \left[\frac{100 \cdot \left(Q^{\text{future climate}}_{\text{future LAI}} - Q^{\text{future climate}}_{\text{historical LAI}} \right)}{Q^{\text{future climate}}_{\text{future LAI}}} \right] \quad (8)$$

where Q_{clim} is the climate effect (CC effect) on streamflow which is due to change in precipitation and temperature only, Q_{net} is climate and LAI effect (CC + LAI effect) on streamflow which is due to change in precipitation, temperature and LAI; and Q_{lai} is the proportion of CC effect on streamflow which is offset by change in LAI due to climate change.

3 Results

This section provides results from the modelling exercises: first, the recently observed prolonged drought and the projected future possible change in climate input in the study catchments is estimated in Sect. 3.1. Second, the impact on both vegetation productivity (Sect. 3.2) and catchment streamflow (Sect. 3.3) of changes in climate input during the Millennium Drought and projected future climate are provided. These results provide the reader with a comparison of the anticipated future change in climate with the recently observed drought.

HESSD
11, 10593–10633, 2014

3.1 Change in the climate variables from change in climate

3.1.1 Millennium drought

The Millennium Drought brought a decline in the mean annual precipitation over the selected sub-catchments which ranged from 17.9 to 24.1 %, with a mean of 20.9 %, and increases in mean annual temperature which ranged from 0.2 to 0.4 °C, with an average of 0.3 °C over the thirteen sub-catchments (Table 1), as compared to the precipitation and temperature in the period (1983–1995).

3.1.2 Future climate

The mean annual precipitation in 2021–2050 over the selected sub-catchments is projected to decline by 2.9 and 3.7 % under the RCP4.5 and RCP8.5 scenarios respectively. Further decline the mean annual precipitation is projected for 2071–2100 of about 5 and 5.2 % under the RCP4.5 and RCP8.5 scenarios respectively (Table 2). Both were compared with the historical period 1981–2010, which includes the recent observed Millennium Drought (1997–2009). The mean annual temperature is also projected to increase in both future periods and emission scenarios (Table 2).

Most of the projected seasonal precipitation simulations showed a shift towards drier climates in all seasons except summer in both emission scenarios and periods. The variability in the projected mean monthly precipitation among climate models indicates great uncertainty but all climate models clearly deviated from the baseline period (1981–2010), underlining the change signal (Fig. 3). The average of the 38 CMIP5 mean monthly precipitation data over the Goulburn–Broken catchment in RCP4.5 emission scenarios showed declines in most of the months. The decreases were up to 8 % in 2021–2050 and up to 15 % in 2071–2100, whereas the increases in January and February were up to 1 and 2.5 %, respectively (Tables 3 and 4). Similarly, under the RCP8.5 emission scenarios the mean monthly precipitation other than in January and February showed decreases up to 8 % in 2021–2050 and up to 17 % in 2071–2100

HESSD
11, 10593–10633, 2014

(Tables 5 and 6). The simulations for January and February showed increases up to 5 % from the historical baseline in both periods. Some climate models projected very wet future climates while others projected relatively dry climates. There are relatively high uncertainties in the projected mean monthly precipitation results in summer when compared with the mean monthly precipitation in winter among the climates models (Fig. 3). On average the CMIP5 models simulated dry future climates in all months except January and February under all emission scenarios, which indicates a drier future climate is projected over the Goulburn–Broken catchment.

In contrast to precipitation the projected mean monthly temperatures from all CMIP5 runs showed increases (Fig. 3), the average of the mean monthly temperatures of all CMIP5 38 runs increased by about 0.8 °C in winter and by 1 °C in summer in 2021–2050 (Table 3), and by about 1.3 °C in winter and 1.8 °C in summer in 2071–2100 (Table 4) under RCP4.5 scenarios. Under the RCP8.5 emission scenario the temperatures increased by 1 to 1.5 °C in winter and summer in 2021–2050 (Table 5) and by 2 and 3 °C by the end of the 21st century (Table 6). After increases in temperature the second variable that drives water availability is potential evaporation which is expected to increase among all CMIP5 runs. In the near future period (2021–2050) the averages of all CMIP5 mean monthly reference evapotranspiration increase by 5 to 13 % in both emission scenarios, with the largest change in winter and the smallest in summer. In the future period of 2071–2100, the mean monthly reference evapotranspiration increased by 7 % in summer and 25 % in winter under RCP4.5 emission scenarios, and by 10 % in summer and 28 % in winter under the RCP8.5 emission scenarios.

3.2 Impact on vegetation productivity (LAI) from change in climate

3.2.1 Millennium drought

The effects of the Millennium Drought (1997–2009) on crop LAI were very severe with reductions in mean annual LAI within the spatial range from 38.1 to 48.4 %, with a mean of 42.7 % (Table 1). The reduction in LAI of pasture was between 16.7 and 21.6 %

HESSD
11, 10593–10633, 2014

across the thirteen selected catchments with spatial average of 19.4 % (Table 1). The LAI of trees responded less than crop and pasture, and were in the range 5.7 to 14 %, with a spatial mean of 9.2 % (Table 1). A significant reduction in each cover type also brought an overall decline in vegetation production of the selected catchments which ranged from 5.8 to 17.9 % (Table 1), which is similar to the reduction of the dominant tree land cover type.

3.2.2 Future climate

The changes in the mean monthly LAI of crop, pasture and trees averaged over the whole Goulburn–Broken catchment under future climates is different among the CMIP5 runs and global warming scenarios, and the average simulated monthly LAI showed declines in all three land cover types (Fig. 4). The near future (2021–2050) results for the selected catchments showed that the mean annual LAI of cropland, pasture and tree declined up to 13, 7 and 5.5 % under the RCP4.5 scenarios, and by up to 16, 8 and 6.6 % under the RCP8.5 scenario (Table 2). A further reduction in the mean annual LAI of each land cover was simulated by the end of the 21st century for both emission scenarios (Table 2).

The seasonal effect of projected climate change on the total vegetation productivity for the selected catchments is given in Tables 3–6. Despite similar percentage change in seasonal precipitation and temperature forcing, the mean monthly total LAI across the catchments shows the largest decline in autumn and the smallest decline in spring during both future periods and scenarios. The predicted decline in the mean seasonal total LAI in the period 2021–2050 is by up to 18.8 % in autumn and by up to 10.3 % in spring and similar in the period 2071–2100 under RCP4.5 (Tables 3 and 4). Further reductions in mean seasonal total LAI were simulated with up to 19.7 and 10.7 % reductions in autumn and spring in both future period under the RCP8.5 emission scenario (Tables 5 and 6).

HESSD
11, 10593–10633, 2014

3.3 Impacts on runoff from change in climate

3.3.1 Millennium drought

The total effects of the Millennium Drought in terms of declines in precipitation and increases in temperature as direct inputs to the model on the mean annual streamflow, and the growth-related effects of decreases in precipitation and increases in evapotranspiration as observed by the changes in LAI were simulated. The simulated reductions in the mean annual streamflow during the Millennium Drought (1997–2009) as compared with the relatively normal period (1983–1995) across the selected catchments ranged from 29.7 to 66.3 % with a mean of 50 %. The reductions in LAI following declines in precipitation and increases in reference evapotranspiration increased the mean annual streamflow by 1.3 to 9.2 % of the above direct climate input effect (Table 1 and Fig. 5).

3.3.2 Future climate

The simulation of mean annual runoff responses to projected CMIP5 climates produced similar impact patterns the "Millennium Drought" in terms of their effects on LAI. The average for the 38 CMIP5 simulations under the RCP4.5 scenario produced declines in mean annual runoff due to the change in climate (Q_{clim}) that ranged from 6.8 to 20.3 % in the period 2021–2050, and 11.5 to 30 % for the period 2071–2100 (Table 2 and Fig. 6). For the higher emission scenario (RCP8.5), the reductions were a bit higher – ranging from 8 to 23 % in 2021–2050 and from 14.5 to 35 % by the end the 21st century (Table 2 and Fig. 6). The reductions in runoff due to climate are offset through the LAI effect (Q_{lai}) in a range of about 2.3 to 21.5 % in the near future period and also in the far future period in a range of 2.4 to 19 % under both emission scenarios (Table 2 and Fig. 6).

The climate change, the LAI effect of climate change and the net climate change effect on the mean monthly runoff for the selected catchments are given in Tables 3–6.

HESSD
11, 10593–10633, 2014

For example, Catchment 6 is located in a high annual precipitation zone with tree as the dominant vegetation cover; whereas catchments 10 and 11 are covered sparsely with trees and have low annual precipitation. In 2021–2050 the reduction in mean monthly runoff (Q_{net}) reached up to 10, 24, and 34 % for catchment 6, 10, and 11, respectively. The results were similar for RCP4.5 and RCP8.5. Further reductions projected by the end of the 21st century were up to 17, 37 and 52 % for catchments 6, 10, and 11, respectively, under both scenarios (Figs. 7 and 8). Catchment 6 showed the lowest seasonality effects from climate change under both emission scenarios and also the LAI effects of climate change showed the smallest variation across seasons. Catchment 11 was found to be the most impacted from projected climate changes and had the greatest benefit from LAI effects of climate change under both emission scenarios and future periods. Between the emissions scenarios the LAI effects of climate change are larger when dry and smaller when wet under RCP8.5 than RCP4.5 but the seasonal pattern is the same.

The uncertainty related to GCM inputs for climate projections on simulated mean annual runoff and the LAI effects of climate change on the mean annual runoff are shown in (Figs. 9 and 10) respectively. Generally, the simulated LAI effects of the climate change showed smaller variation than the climate change as a direct input into the model on mean annual runoff among the CMPI5 runs.

4 Discussion and conclusion

This study investigated the importance of incorporating the effects of climate change, in terms of mean annual precipitation and temperature, on vegetation LAI into hydrological models to estimate changes in mean monthly and mean annual runoff in the Goulburn–Broken catchment, south-eastern Australia.

A combination of VIC hydrological simulations with a simple model that relates climatic fluctuations with LAI for three different vegetation types revealed that 21st century climate change impacts on vegetation productivity (LAI) will significantly

HESSD
11, 10593–10633, 2014

influence the runoff at the study catchment. LAIs of forest, pasture and crop were predicted to decline in the 21st century due to reductions of precipitation along with increases in temperature (Tesemma et al., 2014a). Hence, transpiration from vegetation and evaporative losses from canopy interception would be reduced, which possibly leaves the soil relatively wetter. This is important for runoff generation process as it promotes saturation excess runoff, which is the dominant cause of runoff generation in the study region (Western et al., 1999). Previous studies in the region (Chiew et al., 2009, 2011; Teng et al., 2012a, b) concluded that runoff would decrease due to increases in evaporative demand and decreases in precipitation as a result of ongoing warming in the 21st century. However, the relationship between vegetation productivity and climate fluctuations was not taken into account in their modelling experiments. Therefore, in these studies the LAI effect is ignored and there is consequent overestimation of the runoff decline in the range of 2 to 22 % (Fig. 6).

Projections of climate-induced vegetation dynamics and their hydrological impacts are influenced by various sources of uncertainties that arise from inputs from downscaled GCM outputs. These include large uncertainties in projections for precipitation from the various CMIP5 simulations (Teng et al., 2012b). Besides, most climate models are of different grid scales, and the locations of grid points vary from climate model to climate model. In addition, whereas the temperature is projected to consistently increase across all seasons and CMIP5 simulations, the method used to downscale the GCM outputs can only capture the mean, and the variability which has an effect on the projected future runoff is ignored. Hence the ensemble from 38 CMIP5 simulations of 15 GCMs was used to determine the range of the uncertainty. The results showed that the range of future climate projections from the various GCMs is wide, one climate model could project a very wet future climate while another relatively dry climate, and so on. In future research, a more appropriate approach would be to apply the downscaled climate change scenarios of several CMIP5 runs from selected GCM models individually to the study area to get a sense of the possible range of climate change impact on both LAI then into streamflow.

HESSD
11, 10593–10633, 2014

In interpreting the results presented here it is important to examine the assumptions that were made and the extent to which the results are dependent on those assumptions. Changes in atmospheric CO_2 concentrations could affect vegetation (LAI and narrowing stomata) in addition to warming. One assumption was that the effects of rising atmospheric CO_2 concentrations on vegetation productivity (LAI) and stomatal conductance were not considered. The first is a physiological effect on plants as a result of suppression of their stomata so that transpiration rates tend to decrease during carbon assimilation (Ainsworth and Rogers, 2007; Warren et al., 2011). The second is the fertilization effect on plants by increasing their photosynthesis rate resulting in increases in the LAI, which increases transpiration from the canopy (Ainsworth and Rogers, 2007; Ewert, 2004). However, the latter may be limited by the availability of nutrients, particularly nitrogen (Fernández-Martínez et al., 2014; Körner, 2006). Most of the results on this effect are derived from point experiments which could not be extrapolated to the catchment scale where there is a complex interaction between vegetation, climate and hydrology. In addition at canopy scale the evapotranspiration effect of increased LAI can be masked by shading among leaves, soil cover and raised canopy humidity (Hikosaka et al., 2005; Bunce, 2004). A study that considered both effects suggested that the fertilization effect of rising CO_2 is larger than the stomatal pore reduction effect, and the net effect is decreases in runoff (Piao et al., 2007). These two effects of increasing atmospheric CO_2 concentrations are in opposite directions and may cancel each other if they are close in magnitude, or if the net effect is very small not exceeding 5 % (Gerten et al., 2008). Hence, exclusion of the fertilization and suppression effects on stomata of rising atmospheric CO_2 on vegetation may not change the results.

The other main assumption was that the effect of climate change on the plant functional type was kept constant which allow high level grouping of vegetation for instance pasture represents the various species which might respond to climate change differently. Including this effect in the model could probably improve the results but it is unlikely that there are long term data available to model its effects (if any).

HESSD
11, 10593–10633, 2014

In summary, due to the strong relationship between climatic variation and LAI, hydrological models should incorporate this interaction for improving climate impact assessment. The approach developed in this study can be applied to assess the potential impact of climate changes upon catchment surface water resources.

Acknowledgements. This study was funded by the Australian Research Council (ARC) (Project Nos.: ARC LP100100546, and ARC FT120100130), the Natural Science Foundation of China (Project No.: 91125007) and the Commonwealth of Australia under the Australia China Science and Research Fund (Project No.: ACSRF800). We would like to thank the University of Melbourne for providing a scholarship to the first author.

References

Ainsworth, E. A. and Rogers, A.: The response of photosynthesis and stomatal conductance to rising [CO_2]: mechanisms and environmental interactions, Plant Cell Environ., 30, 258–270, doi:10.1111/j.1365-3040.2007.01641.x, 2007.

Bunce, J. A.: Carbon dioxide effects on stomatal responses to the environment and water use by crops under field conditions, Oecologia, 140, 1–10, doi:10.1007/s00442-003-1401-6, 2004.

Cai, W. and Cowan, T.: Evidence of impacts from rising temperature on inflows to the Murray–Darling Basin, Geophys. Res. Lett., 35, L07701, doi:10.1029/2008GL033390, 2008.

Chiew, F. H. S., Teng, J., Vaze, J., Post, D. A., Perraud, J. M., Kirono, D. G. C., and Viney, N. R.: Estimating climate change impact on runoff across southeast Australia: method, results, and implications of the modeling method, Water Resour. Res., 45, W10414, doi:10.1029/2008WR007338, 2009.

Chiew, F. H. S., Young, W. J., Cai, W., and Teng, J.: Current drought and future hydroclimate projections in southeast Australia and implications for water resources management, Stoch. Environ. Res. Risk A., 25, 601–612, doi:10.1007/s00477-010-0424-x, 2011.

Chiew, F. H. S., Potter, N. J., Vaze, J., Petheram, C., Zhang, L., Teng, J., and Post, D. A.: Observed hydrologic non-stationarity in far south-eastern Australia: implications for modelling and prediction, Stoch. Environ. Res. Risk A., 28, 3–15, 2014.

Ellis, T. W. and Hatton, T. J.: Relating leaf area index of natural eucalypt vegetation to climate variables in southern Australia, Agr. Water Manage., 95, 743–747, doi:10.1016/j.agwat.2008.02.007, 2008.

HESSD

11, 10593–10633, 2014

Ewert, F.: Modelling plant responses to elevated CO_2: how important is leaf area index?, Ann. Bot., 93, 619–627, doi:10.1093/aob/mch101, 2004.
Fernández-Martínez, M., Vicca, S., Janssens, I., Sardans, J., Luyssaert, S., Campioli, M., Chapin III, F., Ciais, P., Malhi, Y., and Obersteiner, M.: Nutrient availability as the key regulator of global forest carbon balance, Nat. Clim. Change, 4, 471–476, 2014.
Gerten, D., Rost, S., von Bloh, W., and Lucht, W.: Causes of change in 20th century global river discharge, Geophys. Res. Lett., 35, L20405, doi:10.1029/2008GL035258, 2008.
Hikosaka, K., Onoda, Y., Kinugasa, T., Nagashima, H., Anten, N. P. R., and Hirose, T.: Plant responses to elevated CO_2 concentration at different scales: leaf, whole plant, canopy, and population, Ecol. Res., 20, 243–253, doi:10.1007/s11284-005-0041-1, 2005.
Hughes, J. D., Petrone, K. C., and Silberstein, R. P.: Drought, groundwater storage and stream flow decline in southwestern Australia, Geophys. Res. Lett., 39, L03408, doi:10.1029/2011GL050797, 2012.
Jahan, N. and Gan, T. Y.: Modelling the vegetation–climate relationship in a boreal mixedwood forest of Alberta using normalized difference and enhanced vegetation indices, Int. J. Remote Sens., 32, 313–335, doi:10.1080/01431160903464146, 2011.
Körner, C.: Plant CO_2 responses: an issue of definition, time and resource supply, New Phytol., 172, 393–411, doi:10.1111/j.1469-8137.2006.01886.x, 2006.
Lockart, N., Kavetski, D., and Franks, S. W.: On the recent warming in the Murray–Darling Basin: land surface interactions misunderstood, Geophys. Res. Lett., 36, L24405, doi:10.1029/2009GL040598, 2009.
Meinshausen, M., Smith, S. J., Calvin, K., Daniel, J. S., Kainuma, M. L. T., Lamarque, J. F., Matsumoto, K., Montzka, S. A., Raper, S. C. B., Riahi, K., Thomson, A., Velders, G. J. M., and van Vuuren, D. P. P.: The RCP greenhouse gas concentrations and their extensions from 1765 to 2300, Climatic Change, 109, 213–241, doi:10.1007/s10584-011-0156-z, 2011.
Milly, P. C. D., Dunne, K. A., and Vecchia, A. V.: Global pattern of trends in streamflow and water availability in a changing climate, Nature, 438, 347–350, 2005.
Moss, R. H., Edmonds, J. A., Hibbard, K. A., Manning, M. R., Rose, S. K., van Vuuren, D. P., Carter, T. R., Emori, S., Kainuma, M., Kram, T., Meehl, G. A., Mitchell, J. F. B., Nakicenovic, N., Riahi, K., Smith, S. J., Stouffer, R. J., Thomson, A. M., Weyant, J. P., and Wilbanks, T. J.: The next generation of scenarios for climate change research and assessment, Nature, 463, 747–756, doi:10.1038/nature08823, 2010.

HESSD
11, 10593–10633, 2014

Murray, S. J., Foster, P. N., and Prentice, I. C.: Evaluation of global continental hydrology as simulated by the Land-surface Processes and eXchanges Dynamic Global Vegetation Model, Hydrol. Earth Syst. Sci., 15, 91–105, doi:10.5194/hess-15-91-2011, 2011.

Murray, S. J., Foster, P. N., and Prentice, I. C.: Future global water resources with respect to climate change and water withdrawals as estimated by a dynamic global vegetation model, J. Hydrol., 448–449, 14–29, doi:10.1016/j.jhydrol.2012.02.044, 2012.

Murray, S. J., Watson, I. M., and Prentice, I. C.: The use of dynamic global vegetation models for simulating hydrology and the potential integration of satellite observations, Prog. Phys. Geog., 37, 63–97, doi:10.1177/0309133312460072, 2013.

O'Grady, A. P., Carter, J. L., and Bruce, J.: Can we predict groundwater discharge from terrestrial ecosystems using existing eco-hydrological concepts?, Hydrol. Earth Syst. Sci., 15, 3731–3739, doi:10.5194/hess-15-3731-2011, 2011.

Palmer, A. R., Fuentes, S., Taylor, D., Macinnis-Ng, C., Zeppel, M., Yunusa, I., and Eamus, D.: Towards a spatial understanding of water use of several land-cover classes: an examination of relationships amongst pre-dawn leaf water potential, vegetation water use, aridity and MODIS LAI, Ecohydrology, 3, 1–10, doi:10.1002/eco.63, 2010.

Peel, M. C. and Blöschl, G.: Hydrological modelling in a changing world, Prog. Phys. Geogr., 35, 249–261, doi:10.1177/0309133311402550, 2011.

Piao, S., Friedlingstein, P., Ciais, P., de Noblet-Ducoudré, N., Labat, D., and Zaehle, S.: Changes in climate and land use have a larger direct impact than rising CO_2 on global river runoff trends, P. Natl. Acad. Sci., 104, 15242–15247, doi:10.1073/pnas.0707213104, 2007.

Potter, N. J. and Chiew, F. H. S.: An investigation into changes in climate characteristics causing the recent very low runoff in the southern Murray–Darling Basin using rainfall–runoff models, Water Resour. Res., 47, W00G10, doi:10.1029/2010WR010333, 2011.

Roderick, M. L. and Farquhar, G. D.: A simple framework for relating variations in runoff to variations in climatic conditions and catchment properties, Water Resour. Res., 47, W00G07, doi:10.1029/2010WR009826, 2011.

Taylor, K. E., Stouffer, R. J., and Meehl, G. A.: An overview of CMIP5 and the experiment design, B. Am. Meteorol. Soc., 93, 485–498, doi:10.1175/BAMS-D-11-00094.1, 2012.

Teng, J., Chiew, F. H. S., Vaze, J., Marvanek, S., and Kirono, D. G. C.: Estimation of climate change impact on mean annual runoff across Continental Australia using Budyko and Fu equations and hydrological models, J. Hydrometeorol, 13, 1094–1106, 2012a.

HESSD
11, 10593–10633, 2014

Teng, J., Vaze, J., Chiew, F. H. S., Wang, B., and Perraud, J.-M.: Estimating the relative uncertainties sourced from GCMs and hydrological models in modeling climate change impact on runoff, J. Hydrometeorol, 13, 122–139, doi:10.1175/JHM-D-11-058.1, 2012b.

Tesemma, Z. K., Wei, Y., Western, A. W., and Peel, M. C.: Leaf area index variation for cropland, pasture and tree in response to climatic variation in the Goulburn–Broken catchment, Australia, J. Hydrometeorol., 15, 1592–1606, doi:10.1175/JHM-D-13-0108.1, 2014a.

Tesemma, Z. K., Wei, Y., Peel, M. C., and Western, A. W.: Effect of year-to-year variability of leaf area index on variable infiltration capacity model performance and simulation of streamflow during drought, Hydrol. Earth Syst. Sci. Discuss., 11, 10515–10552, doi:10.5194/hessd-11-10515-2014, 2014b.

Vaze, J. and Teng, J.: Future climate and runoff projections across New South Wales, Australia: results and practical applications, Hydrol. Process., 25, 18–35, doi:10.1002/hyp.7812, 2011.

Vaze, J., Post, D. A., Chiew, F. H. S., Perraud, J. M., Viney, N. R., and Teng, J.: Climate non-stationarity – validity of calibrated rainfall–runoff models for use in climate change studies, J. Hydrol., 394, 447–457, doi:10.1016/j.jhydrol.2010.09.018, 2010.

Verdon-Kidd, D. C. and Kiem, A. S.: Nature and causes of protracted droughts in southeast Australia: comparison between the Federation, WWII, and Big Dry droughts, Geophys. Res. Lett., 36, L22707, doi:10.1029/2009GL041067, 2009.

Vuuren, D. P., Edmonds, J., Kainuma, M., Riahi, K., Thomson, A., Hibbard, K., Hurtt, G. C., Kram, T., Krey, V., Lamarque, J.-F., Masui, T., Meinshausen, M., Nakicenovic, N., Smith, S. J., and Rose, S. K.: The representative concentration pathways: an overview, Climatic Change, 109, 5–31, 2011.

Warren, J. M., Norby, R. J., and Wullschleger, S. D.: Elevated CO_2 enhances leaf senescence during extreme drought in a temperate forest, Tree Physiol., 31, 117–130, doi:10.1093/treephys/tpr002, 2011.

Western, A. W., Grayson, R. B., and Green, T. R.: The Tarrawarra project: high resolution spatial measurement, modelling and analysis of soil moisture and hydrological response, Hydrol. Process., 13, 633–652, 1999.

White, D. A., Battaglia, M., Mendham, D. S., Crombie, D. S., Kinal, J. O. E., and McGrath, J. F.: Observed and modelled leaf area index in Eucalyptus globulus plantations: tests of optimality and equilibrium hypotheses, Tree Physiol., 30, 831–844, doi:10.1093/treephys/tpq037, 2010.

HESSD
11, 10593–10633, 2014

Table 1. Impacts on mean annual vegetation productivity and streamflow during the Millennium Drought (1997–2009).

Variables*	Catchments ID 1	2	3	4	5	6	7	8	9	10	11	12	13
Crop cover (%)	0.57	1.04									1.52	1.16	1.15
Pasture cover (%)	14.4	32.7	3.26	6.4	0.92	5.5	9.94	2.57	25.9	7.62	63.5	56.3	48.8
Tree cover (%)	85	66.3	96.7	93.6	99.1	94.5	90.1	97.4	74.1	92.4	35	42.6	50.1
P (%)	−23.21	−23.57	−21.08	−17.97	−17.91	−21.02	−20.08	−20.10	−19.42	−21.67	−19.53	−22.56	−24.07
T (°C)	0.19	0.34	0.34	0.38	0.37	0.27	0.32	0.19	0.29	0.24	0.28	0.32	0.29
LAI crop (%)	−44.16	−47.99									−38.11	−41.77	−41.37
LAI pasture (%)	−20.48	−21.60	−19.51	−16.86	−16.68	−18.67	−18.97	−19.11	−19.54	−19.70	−19.60	−20.24	−20.84
LAI tree (%)	−11.38	−10.30	−8.22	−6.62	−5.68	−5.89	−7.01	−6.30	−9.11	−9.21	−14.00	−12.49	−13.92
LAI total (%)	−12.88	−14.39	−8.59	−7.28	−5.78	−6.59	−8.20	−6.63	−11.81	−10.01	−17.92	−17.19	−17.61
Q_{clim} (%)	−49.27	−61.47	−43.65	−39.07	−42.94	−29.71	−43.99	−41.15	−55.17	−57.09	−66.32	−61.80	−57.91
Q_{net} (%)	−48.01	−59.70	−42.77	−38.26	−42.31	−29.33	−43.19	−40.59	−53.26	−55.22	−61.41	−56.10	−53.16
Q_{lai} (%)	2.54	2.88	2.01	2.08	1.48	1.26	1.82	1.36	3.46	3.27	7.40	9.21	8.21

* P (%) is the change in mean annual precipitation in percentage, T (°C) is the change in mean annual temperature in °C, Q_{clim} indicates the climate effect on runoff, Q_{net} is the net effect of climate and LAI on runoff and Q_{lai} is proportion of the climate effect (Q_{clim}) that is offset by the LAI effect.

HESSD
11, 10593–10633, 2014

Table 2. Impacts on mean annual vegetation productivity and streamflow of projected climate change averaged over 38 CMIP5 runs.

Periods	Variables*	Catchments ID 1	2	3	4	5	6	7	8	9	10	11	12	13
2021–2050 RCP4.5	P (%)	−2.9	−2.9	−2.9	−2.9	−2.9	−2.9	−2.9	−2.9	−2.9	−2.9	−2.9	−2.9	−2.9
	T (°C)	0.9	0.9	0.9	0.9	0.9	0.9	0.9	0.9	0.9	0.9	0.9	0.9	0.9
	LAI crop (%)	−12.9	−13.0									−12.9	−13.0	−12.8
	LAI pasture (%)	−5.9	−5.6	−5.4	−5.6	−5.3	−4.8	−5.4	−5.4	−6.1	−6.1	−6.7	−6.3	−6.3
	LAI tree (%)	−3.9	−2.9	−2.5	−2.4	−2.0	−1.7	−2.1	−1.9	−3.0	−3.0	−5.4	−4.6	−4.8
	LAI total (%)	−4.2	−3.9	−2.6	−2.6	−2.0	−1.8	−2.5	−1.9	−3.8	−3.2	−6.3	−5.6	−5.7
	Q_{clim} (%)	−12.3	−17.6	−11.4	−11.5	−13.5	−6.8	−12.4	−12.6	−17.4	−18.4	−20.3	−18.9	−14.2
	Q_{net} (%)	−11.4	−16.3	−10.9	−11.1	−13.2	−6.6	−11.9	−12.2	−15.8	−17.0	−16.3	−14.8	−11.7
	Q_{lai} (%)	7.4	7.7	3.6	3.5	2.7	2.3	4.0	3.2	9.1	7.7	19.5	21.5	17.3
2021–2050 RCP8.5	P (%)	−3.7	−3.7	−3.7	−3.7	−3.7	−3.7	−3.7	−3.7	−3.7	−3.7	−3.7	−3.7	−3.7
	T (°C)	1.2	1.2	1.2	1.2	1.2	1.2	1.2	1.2	1.2	1.2	1.2	1.2	1.2
	LAI crop (%)	−15.7	−15.7									−15.7	−15.7	−15.5
	LAI pasture (%)	−7.2	−6.9	−6.7	−6.8	−6.5	−5.9	−6.6	−6.6	−7.4	−7.5	−8.1	−7.7	−7.7
	LAI tree (%)	−4.8	−3.7	−3.1	−3.0	−2.5	−2.1	−2.7	−2.3	−3.7	−3.7	−6.6	−5.6	−5.9
	LAI total (%)	−5.2	−4.8	−3.3	−3.2	−2.5	−2.3	−3.1	−2.4	−4.7	−4.0	−7.7	−6.9	−6.9
	Q_{clim} (%)	−14.6	−20.7	−13.7	−13.8	−16.3	−8.3	−14.8	−15.0	−20.1	−21.3	−23.3	−21.4	−16.1
	Q_{net} (%)	−13.6	−19.2	−13.2	−13.3	−15.8	−8.1	−14.3	−14.5	−18.3	−19.7	−19.0	−17.0	−13.4
	Q_{lai} (%)	7.2	7.4	3.7	3.6	2.7	2.4	4.0	3.2	8.9	7.5	18.5	20.6	16.8
2071–2100 RCP4.5	P (%)	−5.0	−5.0	−5.0	−5.0	−5.0	−5.0	−5.0	−5.0	−5.0	−5.0	−5.0	−5.0	−5.0
	T (°C)	1.6	1.6	1.6	1.6	1.6	1.6	1.6	1.6	1.6	1.6	1.6	1.6	1.6
	LAI crop (%)	−21.1	−21.3									−20.8	−21.0	−20.7
	LAI pasture (%)	−9.8	−9.5	−9.2	−9.4	−9.0	−8.2	−9.2	−9.2	−10.2	−10.3	−11.0	−10.4	−10.5
	LAI tree (%)	−6.6	−5.1	−4.4	−4.2	−3.5	−3.0	−3.9	−3.4	−5.3	−5.3	−9.2	−7.8	−8.2
	LAI total (%)	−7.2	−6.7	−4.6	−4.5	−3.6	−3.3	−4.4	−3.5	−6.6	−5.7	−10.5	−9.4	−9.5
	Q_{clim} (%)	−19.7	−27.5	−18.6	−18.8	−22.1	−11.5	−20.3	−20.7	−26.9	−28.1	−30.1	−27.7	−21.7
	Q_{net} (%)	−18.3	−25.7	−17.9	−18.1	−21.6	−11.2	−19.6	−20.1	−24.7	−26.2	−25.2	−22.5	−18.6
	Q_{lai} (%)	6.8	6.7	3.6	3.6	2.6	2.4	3.8	3.1	8.1	6.9	16.3	18.9	14.2
2071–2100 RCP8.5	P (%)	−5.2	−5.2	−5.2	−5.2	−5.2	−5.2	−5.2	−5.2	−5.2	−5.2	−5.2	−5.2	−5.2
	T (°C)	2.5	2.5	2.5	2.5	2.5	2.5	2.5	2.5	2.5	2.5	2.5	2.5	2.5
	LAI crop (%)	−28.3	−28.3									−28.5	−28.5	−28.1
	LAI pasture (%)	−13.6	−13	−12.5	−12.9	−12.2	−11.1	−12.5	−12.5	−14	−14.1	−15.4	−14.6	−14.7
	LAI tree (%)	−9.51	−7.37	−6.34	−6.04	−5.09	−4.29	−5.54	−4.84	−7.57	−7.64	−13.2	−11.2	−11.8
	LAI total (%)	−10.2	−9.4	−6.5	−6.5	−5.2	−4.7	−6.2	−5.0	−9.2	−8.1	−14.9	−13.3	−13.4
	Q_{clim} (%)	−24.0	−33.5	−23.9	−24.2	−27.4	−14.5	−25.0	−25.6	−32.0	−33.0	−35.1	−32.8	−25.3
	Q_{net} (%)	−22.3	−31.3	−23.0	−23.3	−26.7	−14.1	−24.0	−24.8	−29.4	−30.8	−29.2	−26.4	−21.7
	Q_{lai} (%)	7.2	6.5	3.8	3.8	2.7	2.7	3.9	3.3	8.2	6.8	16.8	19.4	14.0

* P (%) is the change in mean annual precipitation in percentage, T (°C) is the change in mean annual temperature in °C, Q_{clim} indicates the climate effect on runoff, Q_{net} is the net effect of climate and LAI on runoff and Q_{lai} is proportion of the climate effect (Q_{clim}) that is offset by the LAI effect.

HESSD
11, 10593–10633, 2014

Table 3. Impacts on mean monthly vegetation productivity and streamflow of projected climate change under the RCP4.5 scenario for the period 2021–2050 averaged from the 38 CMIP5 runs.

ID	Variables*	Jan	Feb	Mar	Apr	May	Jun	Jul	Aug	Sep	Oct	Nov	Dec
	P (%)	0.4	1.0	−0.9	−3.6	−4.0	−1.2	−1.2	−2.8	−4.4	−7.7	−4.4	−1.2
	T (°C)	1.1	1.1	1.0	1.0	0.9	0.8	0.8	0.8	0.9	1.0	1.1	1.2
1	LAI total (%)	−9.4	−9.8	−13.2	−12.8	−12.9	−10.9	−10.4	−11.2	−8.2	−7.3	−6.1	−7.1
	Q_{clim} (%)	−10.8	−10.3	−10.4	−10.9	−11.0	−8.4	−8.5	−11.2	−13.1	−19.9	−15.7	−12.4
	Q_{net} (%)	−9.7	−9.2	−9.3	−9.8	−10.1	−7.5	−7.6	−10.3	−12.3	−19.1	−14.8	−11.5
	Q_{lai} (%)	9.6	10.6	10.1	9.4	8.6	10.8	10.0	8.1	6.4	4.3	5.6	7.4
2	LAI total (%)	−12.1	−12.3	−15.6	−15.3	−15.4	−12.4	−13.1	−13.1	−10.1	−9.5	−8.7	−11.0
	Q_{clim} (%)	−12.8	−7.6	−6.4	−8.1	−11.5	−11.2	−14.1	−18.3	−21.1	−23.8	−20.7	−16.8
	Q_{net} (%)	−11.5	−6.4	−5.5	−7.1	−10.5	−10.3	−13.0	−16.7	−19.3	−22.4	−19.4	−15.5
	Q_{lai} (%)	10.2	14.7	14.2	11.8	8.2	7.6	7.6	8.6	8.3	6.1	6.2	7.3
3	LAI total (%)	−6.3	−7.7	−10.8	−11.1	−10.2	−9.3	−9.0	−8.5	−5.9	−5.2	−4.5	−5.0
	Q_{clim} (%)	−7.9	−2.9	−3.5	−6.8	−10.6	−10.7	−9.1	−8.8	−10.4	−17.5	−18.2	−14.4
	Q_{net} (%)	−7.7	−2.6	−3.2	−6.5	−10.0	−10.0	−8.4	−8.4	−10.1	−17.3	−17.9	−14.2
	Q_{lai} (%)	3.2	10.6	8.5	5.5	5.3	6.5	6.9	5.2	3.0	1.6	1.5	1.6
4	LAI total (%)	−5.6	−6.4	−9.1	−10.2	−9.6	−8.3	−7.0	−6.5	−4.7	−4.2	−3.7	−4.2
	Q_{clim} (%)	−7.4	−2.7	−3.0	−6.3	−8.6	−11.3	−11.1	−9.7	−10.0	−16.0	−18.8	−15.2
	Q_{net} (%)	−7.1	−2.4	−2.7	−6.0	−8.1	−10.6	−10.4	−9.2	−9.7	−15.7	−18.5	−15.0
	Q_{lai} (%)	3.6	11.1	10.9	5.3	5.7	6.2	6.0	4.5	2.8	1.6	1.4	1.6
5	LAI total (%)	−4.2	−5.3	−7.2	−8.6	−7.6	−7.0	−5.7	−5.1	−3.7	−3.1	−2.7	−2.9
	Q_{clim} (%)	−7.6	−5.8	−7.2	−10.4	−11.9	−12.6	−13.7	−14.3	−13.6	−17.6	−14.5	−10.3
	Q_{net} (%)	−7.4	−5.4	−6.8	−10.0	−11.4	−12.2	−13.2	−13.9	−13.2	−17.4	−14.3	−10.1
	Q_{lai} (%)	3.7	5.6	5.0	3.8	3.8	3.5	3.6	3.1	2.6	1.5	1.6	2.0
6	LAI total (%)	−5.0	−6.3	−8.2	−9.4	−8.7	−7.6	−6.6	−5.5	−4.3	−3.7	−3.2	−3.6
	Q_{clim} (%)	−6.9	−4.9	−4.7	−6.2	−7.7	−5.7	−4.7	−5.2	−6.6	−8.9	−10.1	−8.6
	Q_{net} (%)	−6.8	−4.7	−4.5	−6.0	−7.4	−5.4	−4.5	−5.1	−6.5	−8.8	−10.0	−8.5
	Q_{lai} (%)	2.1	3.6	4.6	4.5	4.4	4.6	3.9	2.5	1.6	1.2	1.2	1.4
7	LAI total (%)	−6.7	−7.9	−9.8	−10.7	−9.8	−8.5	−7.7	−6.6	−5.3	−4.5	−4.2	−5.0
	Q_{clim} (%)	−7.3	−5.6	−6.4	−9.3	−10.2	−10.9	−11.6	−13.3	−14.0	−17.6	−14.0	−10.0
	Q_{net} (%)	−6.8	−5.1	−5.8	−8.8	−9.6	−10.4	−11.0	−12.8	−13.5	−17.2	−13.6	−9.6
	Q_{lai} (%)	6.6	9.2	8.2	5.8	5.5	4.9	5.0	4.3	3.6	2.3	2.8	3.7

HESSD
11, 10593–10633, 2014

Table 3. Continued.

ID	Variables*	Jan	Feb	Mar	Apr	May	Jun	Jul	Aug	Sep	Oct	Nov	Dec
8	LAI total (%)	−5.2	−6.6	−8.3	−9.1	−8.1	−7.3	−6.7	−5.6	−4.4	−3.7	−3.3	−3.7
	Q_{clim} (%)	−11.9	−12.8	−13.6	−14.4	−15.0	−12.6	−11.5	−11.4	−12.7	−13.6	−12.0	−11.1
	Q_{net} (%)	−11.4	−12.4	−13.2	−14.0	−14.5	−12.2	−11.1	−11.0	−12.3	−13.2	−11.7	−10.8
	Q_{lai} (%)	3.4	3.3	3.1	2.9	3.0	3.3	3.6	3.4	2.9	2.7	3.1	3.4
9	LAI total (%)	−11.2	−11.9	−13.6	−13.2	−11.9	−9.2	−8.6	−8.2	−7.2	−7.0	−7.0	−8.9
	Q_{clim} (%)	−9.4	−6.9	−7.3	−11.6	−12.2	−14.8	−16.6	−18.2	−19.4	−24.3	−19.8	−14.7
	Q_{net} (%)	−8.1	−5.5	−6.0	−10.3	−10.9	−13.1	−14.6	−16.3	−17.6	−22.9	−18.6	−13.5
	Q_{lai} (%)	14.0	20.4	18.6	11.5	10.8	11.4	11.9	10.1	9.2	5.4	6.1	8.0
10	LAI total (%)	−8.7	−10.0	−12.9	−12.0	−10.6	−8.8	−8.1	−7.6	−6.0	−5.6	−5.3	−6.1
	Q_{clim} (%)	−18.8	−13.7	−10.6	−10.4	−12.5	−10.9	−13.3	−17.1	−21.9	−26.0	−22.9	−20.6
	Q_{net} (%)	−17.3	−12.2	−9.3	−9.3	−11.3	−9.9	−12.1	−15.5	−20.3	−24.4	−21.5	−19.2
	Q_{lai} (%)	7.8	11.0	12.4	10.9	10.3	9.0	9.4	9.1	7.4	6.1	6.3	7.0
11	LAI total (%)	−18.1	−17.3	−17.9	−16.1	−17.5	−12.9	−12.0	−13.0	−11.5	−12.4	−10.1	−14.3
	Q_{clim} (%)	0.4	6.4	−0.7	−8.8	−8.3	−3.7	−10.2	−19.2	−28.7	−38.8	−35.6	−29.1
	Q_{net} (%)	0.6	6.6	−0.6	−8.7	−8.2	−3.2	−6.4	−13.8	−22.9	−34.3	−31.6	−25.4
	Q_{lai} (%)	−47.1	−2.1	18.2	0.9	0.5	14.8	36.6	28.2	20.3	11.6	11.4	12.7
12	LAI total (%)	−16.9	−16.2	−18.1	−16.0	−18.3	−13.1	−11.6	−12.7	−10.7	−11.6	−8.8	−12.6
	Q_{clim} (%)	−13.5	−12.0	−11.8	−11.8	−11.5	−9.1	−11.2	−20.9	−25.4	−30.3	−18.8	−16.7
	Q_{net} (%)	−9.7	−7.8	−7.7	−8.3	−8.6	−6.5	−8.0	−15.6	−20.3	−26.1	−15.9	−13.2
	Q_{lai} (%)	28.4	34.5	34.3	29.6	24.9	28.6	28.6	25.3	20.0	13.8	15.8	20.7
13	LAI total (%)	−16.1	−16.1	−18.5	−16.7	−18.5	−13.8	−12.7	−13.6	−11.5	−12.2	−9.7	−12.9
	Q_{clim} (%)	0.2	5.0	1.2	−8.0	−7.8	−5.0	−9.3	−17.4	−22.7	−29.8	−21.2	−9.5
	Q_{net} (%)	0.5	5.5	1.7	−7.8	−7.5	−3.8	−6.6	−13.7	−19.1	−26.6	−19.6	−8.3
	Q_{lai} (%)	−153.3	−8.9	−39.9	2.2	3.5	23.8	28.5	21.6	16.0	10.5	7.5	11.8

* P (%) is the change in mean annual precipitation in percentage, T (°C) is the change in mean annual temperature in °C, Q_{clim} indicates the climate effect on runoff, Q_{net} is the net effect of climate and LAI on runoff and Q_{lai} is proportion of the climate effect (Q_{clim}) that is offset by the LAI effect.

HESSD
11, 10593–10633, 2014

Table 4. Impacts on mean monthly vegetation productivity and streamflow of projected climate under the RCP4.5 scenario for the period 2071–2100 averaged from the 38 CMIP5 runs.

ID	Variables*	Jan	Feb	Mar	Apr	May	Jun	Jul	Aug	Sep	Oct	Nov	Dec
	P (%)	−0.2	2.6	−3.0	−2.6	−4.0	−3.4	−2.8	−5.2	−9.2	−14.5	−7.1	−4.8
	T (°C)	1.8	1.8	1.6	1.6	1.4	1.3	1.3	1.3	1.4	1.7	1.8	1.9
1	LAI total (%)	−9.8	−10.1	−13.7	−13.3	−13.3	−11.3	−10.8	−11.6	−8.5	−7.6	−6.4	−7.5
	Q_{clim} (%)	−18.0	−16.0	−17.3	−15.5	−15.2	−13.6	−13.6	−18.1	−21.7	−31.2	−24.5	−22.8
	Q_{net} (%)	−16.4	−14.4	−15.8	−14.0	−13.7	−12.2	−12.3	−16.7	−20.5	−30.1	−23.2	−21.4
	Q_{lai} (%)	8.6	10.2	8.9	9.8	9.5	10.2	9.5	7.5	5.5	3.6	5.3	6.1
2	LAI total (%)	−12.6	−12.7	−16.0	−15.7	−15.8	−12.9	−13.5	−13.5	−10.5	−9.8	−9.0	−11.3
	Q_{clim} (%)	−20.8	−11.6	−10.8	−10.1	−14.1	−16.9	−21.6	−28.2	−33.3	−38.0	−32.0	−29.2
	Q_{net} (%)	−19.0	−10.0	−9.4	−8.6	−12.6	−15.7	−20.1	−25.9	−31.1	−36.1	−30.2	−27.5
	Q_{lai} (%)	8.9	14.2	12.6	14.4	10.4	7.4	7.0	7.9	6.6	4.9	5.6	5.9
3	LAI total (%)	−6.8	−8.2	−11.6	−11.8	−10.8	−9.9	−9.5	−9.0	−6.2	−5.5	−4.9	−5.5
	Q_{clim} (%)	−14.3	−3.9	−6.7	−7.4	−12.7	−15.4	−14.1	−14.3	−18.5	−29.3	−29.6	−25.5
	Q_{net} (%)	−13.9	−3.3	−6.2	−6.8	−11.8	−14.2	−13.1	−13.5	−18.0	−28.8	−29.2	−25.2
	Q_{lai} (%)	2.8	13.3	7.4	8.4	7.1	7.4	7.4	5.4	2.8	1.4	1.4	1.4
4	LAI total (%)	−6.0	−6.9	−9.7	−10.9	−10.2	−8.9	−7.4	−6.9	−5.0	−4.5	−4.0	−4.5
	Q_{clim} (%)	−13.5	−3.5	−6.1	−6.6	−9.8	−15.9	−16.8	−15.6	−17.6	−28.0	−30.6	−26.6
	Q_{net} (%)	−13.1	−3.0	−5.5	−6.0	−9.0	−14.8	−15.7	−14.8	−17.1	−27.6	−30.2	−26.2
	Q_{lai} (%)	3.2	14.1	9.3	8.6	8.3	7.0	6.6	4.7	2.7	1.4	1.3	1.4
5	LAI total (%)	−4.7	−5.8	−7.9	−9.3	−8.3	−7.5	−6.2	−5.4	−4.0	−3.4	−3.0	−3.2
	Q_{clim} (%)	−14.1	−8.9	−12.6	−13.4	−15.4	−18.9	−21.3	−22.7	−23.2	−30.2	−23.6	−20.1
	Q_{net} (%)	−13.7	−8.3	−12.0	−12.8	−14.6	−18.3	−20.5	−22.0	−22.7	−29.8	−23.3	−19.8
	Q_{lai} (%)	3.5	6.3	4.7	4.9	4.8	3.6	3.6	3.1	2.4	1.3	1.6	1.8
6	LAI total (%)	−5.5	−6.8	−8.9	−10.2	−9.4	−8.2	−7.0	−5.9	−4.6	−4.0	−3.5	−3.9
	Q_{clim} (%)	−12.4	−8.4	−8.5	−8.7	−9.8	−8.6	−7.7	−8.8	−11.5	−15.7	−17.2	−15.7
	Q_{net} (%)	−12.1	−8.1	−8.1	−8.2	−9.3	−8.1	−7.4	−8.6	−11.3	−15.5	−17.0	−15.5
	Q_{lai} (%)	2.0	3.7	4.4	5.6	6.0	5.4	4.2	2.6	1.6	1.1	1.2	1.3
7	LAI total (%)	−7.2	−8.5	−10.5	−11.5	−10.5	−9.1	−8.2	−7.0	−5.6	−4.9	−4.5	−5.4
	Q_{clim} (%)	−13.2	−9.0	−11.2	−12.6	−13.7	−16.9	−18.6	−21.3	−23.5	−29.4	−22.6	−19.3
	Q_{net} (%)	−12.5	−8.1	−10.4	−11.7	−12.8	−16.1	−17.7	−20.4	−22.7	−28.8	−22.0	−18.7
	Q_{lai} (%)	5.9	9.5	7.4	6.8	6.6	5.0	4.8	4.0	3.1	2.0	2.7	3.1

HESSD
11, 10593–10633, 2014

Table 4. Continued.

ID	Variables*	Jan	Feb	Mar	Apr	May	Jun	Jul	Aug	Sep	Oct	Nov	Dec
8	LAI total (%)	−5.7	−7.2	−9.1	−9.9	−8.9	−7.9	−7.2	−6.1	−4.7	−4.0	−3.6	−4.1
	Q_{clim} (%)	−20.5	−21.2	−22.6	−22.3	−22.9	−20.4	−18.5	−18.2	−20.5	−22.8	−20.3	−20.2
	Q_{net} (%)	−19.8	−20.6	−21.9	−21.6	−22.2	−19.7	−17.8	−17.6	−19.9	−22.3	−19.7	−19.6
	Q_{lai} (%)	3.2	3.2	3.0	3.0	3.1	3.3	3.6	3.4	2.9	2.6	3.0	3.1
9	LAI total (%)	−11.8	−12.5	−14.3	−13.8	−12.5	−9.7	−9.0	−8.6	−7.5	−7.3	−7.3	−9.4
	Q_{clim} (%)	−16.5	−10.4	−12.4	−15.0	−15.6	−21.8	−25.3	−27.6	−30.8	−38.2	−30.7	−26.3
	Q_{net} (%)	−14.6	−8.3	−10.4	−13.1	−13.7	−19.5	−22.4	−25.1	−28.5	−36.6	−29.0	−24.6
	Q_{lai} (%)	11.9	20.0	16.1	12.8	12.1	10.8	11.4	9.1	7.3	4.3	5.4	6.4
10	LAI total (%)	−9.4	−10.8	−13.8	−12.7	−11.3	−9.4	−8.6	−8.1	−6.4	−5.9	−5.7	−6.6
	Q_{clim} (%)	−29.5	−20.2	−16.5	−13.7	−15.8	−16.3	−20.0	−25.9	−33.6	−40.0	−34.7	−33.6
	Q_{net} (%)	−27.5	−18.2	−14.6	−12.0	−13.9	−14.9	−18.3	−23.9	−31.4	−37.9	−32.8	−31.7
	Q_{lai} (%)	6.7	9.9	11.3	12.5	12.2	8.6	8.4	8.1	6.4	5.2	5.5	5.5
11	LAI total (%)	−18.4	−17.5	−18.3	−16.5	−17.9	−13.2	−12.3	−13.3	−11.7	−12.6	−10.3	−14.5
	Q_{clim} (%)	−1.6	9.7	−4.8	−8.0	−8.7	−6.5	−15.4	−29.2	−42.6	−56.6	−49.2	−46.3
	Q_{net} (%)	−1.3	10.0	−4.6	−7.8	−8.6	−5.8	−10.6	−21.8	−35.4	−51.7	−44.9	−42.2
	Q_{lai} (%)	18.4	−2.2	3.9	1.6	0.7	9.6	31.5	25.2	16.9	8.6	8.6	8.9
12	LAI total (%)	−17.1	−16.4	−18.3	−16.3	−18.7	−13.4	−11.9	−13.0	−10.9	−11.8	−8.9	−12.7
	Q_{clim} (%)	−20.7	−16.9	−18.0	−15.4	−14.5	−13.8	−16.6	−30.2	−37.0	−44.0	−29.1	−28.0
	Q_{net} (%)	−15.4	−11.2	−12.4	−10.5	−10.5	−10.1	−12.4	−23.5	−31.1	−38.7	−24.9	−23.2
	Q_{lai} (%)	25.7	33.8	30.9	31.8	27.8	27.1	25.7	21.9	15.9	12.0	14.7	16.9
13	LAI total (%)	−16.3	−16.3	−18.8	−17.0	−18.8	−14.2	−13.1	−14.0	−11.8	−12.3	−9.8	−13.1
	Q_{clim} (%)	−1.3	7.2	−2.0	−7.3	−8.5	−8.5	−14.1	−25.0	−35.3	−46.9	−31.7	−22.4
	Q_{net} (%)	−0.9	7.7	−1.3	−7.1	−8.2	−6.9	−10.6	−20.8	−30.6	−42.8	−29.5	−21.1
	Q_{lai} (%)	33.5	−7.9	36.1	3.2	3.6	18.9	24.9	16.8	13.4	8.8	6.9	6.0

* P (%) is the change in mean annual precipitation in percentage, T (°C) is the change in mean annual temperature in °C, Q_{clim} indicates the climate effect on runoff, Q_{net} is the net effect of climate and LAI on runoff and Q_{lai} is proportion of the climate effect (Q_{clim}) that is offset by the LAI effect.

HESSD
11, 10593–10633, 2014

Table 5. Impacts on mean monthly vegetation productivity and streamflow of projected climate under the RCP8.5 scenario for the period 2021–2050 averaged from the 38 CMIP5 runs.

ID	Variables*	Jan	Feb	Mar	Apr	May	Jun	Jul	Aug	Sep	Oct	Nov	Dec
	P (%)	0.3	0.7	−0.4	−1.4	−5.2	−2.2	−1.2	−4.2	−6.9	−8.0	−6.7	−2.2
	T (°C)	1.4	1.3	1.1	1.2	1.1	0.9	1.0	1.0	1.1	1.2	1.4	1.4
1	LAI total (%)	−9.5	−9.9	−13.5	−13.0	−13.1	−11.1	−10.6	−11.3	−8.3	−7.4	−6.2	−7.3
	Q_{clim} (%)	−13.1	−12.9	−12.2	−11.2	−13.1	−10.5	−9.5	−13.8	−16.7	−21.5	−19.4	−15.9
	Q_{net} (%)	−11.9	−11.6	−11.0	−10.0	−12.0	−9.4	−8.5	−12.8	−15.7	−20.6	−18.4	−14.9
	Q_{lai} (%)	9.2	10.0	10.2	10.9	8.6	10.2	10.4	7.5	5.8	4.3	5.3	6.8
2	LAI total (%)	−12.3	−12.4	−15.8	−15.5	−15.6	−12.6	−13.3	−13.2	−10.3	−9.6	−8.9	−11.1
	Q_{clim} (%)	−15.5	−10.1	−6.9	−6.4	−12.6	−13.4	−15.5	−21.9	−26.5	−26.2	−24.9	−20.7
	Q_{net} (%)	−14.0	−8.8	−5.9	−5.3	−11.5	−12.4	−14.2	−20.1	−24.6	−24.5	−23.4	−19.2
	Q_{lai} (%)	9.8	12.7	15.5	18.0	8.9	7.5	7.9	8.0	7.1	6.4	6.0	7.0
3	LAI total (%)	−6.5	−7.9	−11.1	−11.3	−10.5	−9.5	−9.2	−8.7	−6.0	−5.3	−4.7	−5.2
	Q_{clim} (%)	−9.9	−4.3	−3.5	−4.5	−11.1	−12.3	−10.1	−10.8	−14.1	−20.3	−21.6	−18.4
	Q_{net} (%)	−9.6	−4.0	−3.2	−4.1	−10.4	−11.5	−9.4	−10.3	−13.8	−19.9	−21.3	−18.1
	Q_{lai} (%)	3.1	8.6	10.3	10.4	6.1	6.9	7.5	5.1	2.7	1.6	1.5	1.5
4	LAI total (%)	−5.8	−6.6	−9.3	−10.5	−9.9	−8.6	−7.2	−6.6	−4.8	−4.3	−3.8	−4.3
	Q_{clim} (%)	−9.3	−4.2	−3.0	−3.7	−8.8	−12.9	−12.3	−11.9	−13.6	−18.3	−22.4	−19.4
	Q_{net} (%)	−8.9	−3.8	−2.6	−3.2	−8.2	−12.0	−11.5	−11.4	−13.3	−18.0	−22.1	−19.1
	Q_{lai} (%)	3.5	8.7	13.6	11.5	6.8	6.6	6.6	4.5	2.6	1.7	1.4	1.5
5	LAI total (%)	−4.4	−5.5	−7.5	−8.8	−7.9	−7.2	−5.9	−5.2	−3.8	−3.2	−2.8	−3.0
	Q_{clim} (%)	−9.5	−7.8	−8.0	−9.3	−13.5	−14.9	−15.1	−17.3	−18.1	−19.3	−18.5	−13.6
	Q_{net} (%)	−9.2	−7.4	−7.5	−8.8	−12.9	−14.4	−14.6	−16.7	−17.6	−19.0	−18.2	−13.3
	Q_{lai} (%)	3.6	5.2	5.6	5.4	4.1	3.5	3.9	3.0	2.4	1.6	1.6	1.9
6	LAI total (%)	−5.2	−6.5	−8.4	−9.7	−8.9	−7.8	−6.8	−5.6	−4.4	−3.8	−3.3	−3.7
	Q_{clim} (%)	−8.6	−6.4	−5.5	−5.4	−8.1	−6.6	−5.3	−6.5	−8.8	−10.8	−12.3	−10.8
	Q_{net} (%)	−8.5	−6.2	−5.2	−5.0	−7.7	−6.3	−5.1	−6.3	−8.6	−10.6	−12.2	−10.7
	Q_{lai} (%)	2.1	3.5	4.9	6.6	5.2	4.9	4.3	2.5	1.5	1.2	1.2	1.3
7	LAI total (%)	−6.9	−8.1	−10.0	−11.0	−10.1	−8.7	−7.9	−6.8	−5.4	−4.6	−4.3	−5.1
	Q_{clim} (%)	−9.0	−7.3	−7.2	−8.7	−11.6	−13.0	−13.0	−16.1	−18.2	−19.2	−17.6	−12.9
	Q_{net} (%)	−8.4	−6.7	−6.6	−8.1	−11.0	−12.3	−12.3	−15.5	−17.6	−18.8	−17.1	−12.5
	Q_{lai} (%)	6.4	8.6	8.8	7.6	5.8	5.0	5.3	4.1	3.2	2.5	2.7	3.5

HESSD
11, 10593–10633, 2014

Table 5. Continued.

ID	Variables*	Jan	Feb	Mar	Apr	May	Jun	Jul	Aug	Sep	Oct	Nov	Dec
8	LAI total (%)	−5.4	−6.8	−8.6	−9.4	−8.4	−7.5	−6.9	−5.8	−4.5	−3.8	−3.4	−3.9
	Q_{clim} (%)	−14.5	−15.6	−16.2	−16.1	−17.5	−15.0	−13.1	−13.5	−15.6	−15.5	−15.0	−14.0
	Q_{net} (%)	−14.0	−15.1	−15.6	−15.6	−16.9	−14.5	−12.6	−13.0	−15.2	−15.0	−14.5	−13.5
	Q_{lai} (%)	3.4	3.3	3.2	3.2	3.0	3.4	3.8	3.4	2.9	2.8	3.0	3.3
9	LAI total (%)	−11.4	−12.1	−13.9	−13.4	−12.2	−9.4	−8.7	−8.3	−7.3	−7.1	−7.1	−9.1
	Q_{clim} (%)	−11.4	−8.8	−8.2	−10.8	−13.6	−17.1	−18.3	−21.2	−24.4	−25.8	−24.0	−18.3
	Q_{net} (%)	−9.9	−7.2	−6.6	−9.2	−12.0	−15.1	−16.1	−19.2	−22.4	−24.4	−22.6	−16.9
	Q_{lai} (%)	13.4	18.4	19.6	14.7	11.2	11.3	12.4	9.6	7.9	5.6	5.7	7.4
10	LAI total (%)	−9.0	−10.3	−13.3	−12.3	−10.9	−9.1	−8.3	−7.8	−6.2	−5.7	−5.5	−6.3
	Q_{clim} (%)	−22.1	−16.7	−11.7	−8.9	−13.8	−12.8	−14.6	−19.9	−26.5	−28.7	−27.0	−24.9
	Q_{net} (%)	−20.5	−15.1	−10.2	−7.6	−12.2	−11.7	−13.2	−18.2	−24.7	−26.9	−25.4	−23.3
	Q_{lai} (%)	7.4	9.8	12.9	15.3	11.0	8.8	9.8	8.6	6.9	6.3	6.0	6.4
11	LAI total (%)	−18.3	−17.4	−18.1	−16.3	−17.7	−13.0	−12.1	−13.1	−11.5	−12.5	−10.3	−14.4
	Q_{clim} (%)	0.5	4.5	0.6	−3.5	−9.3	−5.0	−10.5	−22.6	−35.1	−41.3	−40.4	−34.2
	Q_{net} (%)	0.7	4.6	0.8	−3.4	−9.3	−4.3	−6.3	−16.8	−28.6	−36.5	−36.2	−30.3
	Q_{lai} (%)	−47.8	−3.6	−23.5	2.9	0.5	13.3	39.8	25.8	18.3	11.8	10.5	11.5
12	LAI total (%)	−17.0	−16.3	−18.3	−16.2	−18.5	−13.2	−11.7	−12.8	−10.8	−11.7	−8.9	−12.7
	Q_{clim} (%)	−15.7	−14.3	−13.2	−11.2	−12.9	−10.9	−11.6	−23.6	−29.9	−32.5	−23.0	−20.4
	Q_{net} (%)	−11.3	−9.6	−8.5	−7.2	−9.7	−7.9	−7.9	−18.4	−24.7	−27.7	−19.4	−16.4
	Q_{lai} (%)	27.8	32.9	35.2	36.1	25.3	27.5	31.8	22.2	17.4	14.8	15.5	19.4
13	LAI total (%)	−16.2	−16.2	−18.7	−16.9	−18.6	−14.0	−12.9	−13.7	−11.6	−12.2	−9.8	−13.0
	Q_{clim} (%)	0.4	3.1	3.2	−3.3	−8.8	−6.6	−9.6	−20.0	−28.2	−31.0	−26.5	−11.2
	Q_{net} (%)	0.7	3.6	3.8	−3.0	−8.5	−5.1	−6.8	−16.3	−24.2	−26.9	−24.5	−9.7
	Q_{lai} (%)	−94.3	−14.4	−20.2	6.2	3.4	22.1	29.1	18.7	14.5	13.3	7.4	13.2

* P (%) is the change in mean annual precipitation in percentage, T (°C) is the change in mean annual temperature in °C, Q_{clim} indicates the climate effect on runoff, Q_{net} is the net effect of climate and LAI on runoff and Q_{lai} is proportion of the climate effect (Q_{clim}) that is offset by the LAI effect.

HESSD
11, 10593–10633, 2014

Table 6. Impacts on mean monthly vegetation productivity and streamflow of projected climate under the RCP8.5 scenario for the period 2071–2100 averaged from the 38 CMIP5 runs.

ID	Variables*	Jan	Feb	Mar	Apr	May	Jun	Jul	Aug	Sep	Oct	Nov	Dec
	P (%)	4.8	4.2	0.2	−5.0	−5.4	−4.2	−5.6	−5.6	−12.5	−16.8	−7.7	−3.2
	T (°C)	2.7	2.6	2.5	2.5	2.3	2.0	2.1	2.1	2.3	2.6	2.8	2.9
1	LAI total (%)	−10.3	−10.6	−14.4	−13.9	−14.0	−11.7	−11.3	−12.1	−8.9	−8.0	−6.7	−7.8
	Q_{clim} (%)	−19.3	−19.2	−19.2	−19.7	−19.1	−16.8	−18.6	−22.3	−28.0	−36.4	−29.5	−26.3
	Q_{net} (%)	−17.2	−17.1	−17.2	−17.7	−17.2	−15.0	−17.0	−20.5	−26.5	−34.9	−27.9	−24.5
	Q_{lai} (%)	10.6	10.8	10.5	9.9	9.8	10.8	9.0	8.0	5.5	3.9	5.7	6.8
2	LAI total (%)	−13.1	−13.2	−16.7	−16.4	−16.4	−13.3	−14.0	−14.0	−10.9	−10.2	−9.4	−11.8
	Q_{clim} (%)	−21.9	−13.2	−9.6	−12.7	−17.5	−20.6	−28.1	−34.7	−41.8	−44.7	−38.1	−33.0
	Q_{net} (%)	−19.7	−11.2	−7.8	−10.8	−15.6	−19.0	−26.4	−32.2	−39.4	−42.5	−35.9	−30.9
	Q_{lai} (%)	10.1	15.2	19.0	15.1	10.9	7.8	6.3	7.3	5.9	4.9	5.7	6.3
3	LAI total (%)	−7.4	−8.8	−12.3	−12.5	−11.5	−10.4	−10.1	−9.5	−6.6	−5.9	−5.3	−5.9
	Q_{clim} (%)	−11.5	−2.9	−3.9	−9.8	−15.6	−18.7	−20.2	−19.7	−25.5	−35.8	−35.5	−28.5
	Q_{net} (%)	−11.0	−2.1	−3.2	−8.9	−14.4	−17.2	−18.8	−18.6	−24.7	−35.2	−35.0	−28.0
	Q_{lai} (%)	4.9	25.4	18.2	8.8	7.8	7.9	6.8	5.5	2.9	1.6	1.5	1.7
4	LAI total (%)	−6.5	−7.4	−10.4	−11.6	−10.9	−9.4	−7.9	−7.3	−5.3	−4.9	−4.4	−4.9
	Q_{clim} (%)	−10.7	−2.7	−3.2	−9.1	−12.7	−19.4	−23.4	−21.0	−24.0	−34.7	−36.6	−29.4
	Q_{net} (%)	−10.0	−2.0	−2.4	−8.3	−11.6	−17.9	−22.0	−20.0	−23.3	−34.2	−36.0	−28.9
	Q_{lai} (%)	5.9	25.6	25.6	8.5	8.7	7.6	6.1	4.9	2.9	1.6	1.4	1.8
5	LAI total (%)	−5.2	−6.3	−8.6	−10.0	−9.0	−8.1	−6.7	−5.9	−4.4	−3.7	−3.3	−3.6
	Q_{clim} (%)	−13.2	−10.8	−12.2	−17.6	−19.4	−22.8	−27.7	−28.3	−30.5	−36.1	−28.7	−22.4
	Q_{net} (%)	−12.5	−9.9	−11.3	−16.7	−18.4	−21.9	−26.8	−27.4	−29.8	−35.6	−28.2	−21.9
	Q_{lai} (%)	5.5	7.5	6.9	4.9	4.9	3.9	3.3	3.1	2.3	1.4	1.9	2.4
6	LAI total (%)	−6.0	−7.4	−9.7	−10.9	−10.1	−8.8	−7.6	−6.4	−5.0	−4.3	−3.8	−4.3
	Q_{clim} (%)	−13.2	−9.5	−8.4	−10.3	−12.2	−10.8	−11.0	−11.8	−15.3	−20.0	−21.3	−18.1
	Q_{net} (%)	−12.8	−9.0	−7.8	−9.6	−11.4	−10.1	−10.6	−11.5	−15.0	−19.8	−21.0	−17.8
	Q_{lai} (%)	2.8	4.8	6.6	6.7	6.7	6.0	4.1	2.8	1.7	1.3	1.3	1.6
7	LAI total (%)	−7.8	−9.1	−11.4	−12.4	−11.4	−9.8	−8.8	−7.6	−6.0	−5.2	−4.9	−5.9
	Q_{clim} (%)	−13.4	−11.2	−12.0	−16.4	−17.4	−20.4	−24.6	−26.3	−30.3	−34.9	−27.4	−21.7
	Q_{net} (%)	−12.3	−10.0	−10.8	−15.2	−16.3	−19.3	−23.5	−25.3	−29.4	−34.1	−26.5	−20.9
	Q_{lai} (%)	8.1	10.3	9.5	6.8	6.7	5.3	4.5	4.1	3.0	2.1	3.0	3.8

HESSD
11, 10593–10633, 2014

Table 6. Continued.

ID	Variables*	Jan	Feb	Mar	Apr	May	Jun	Jul	Aug	Sep	Oct	Nov	Dec
8	LAI total (%)	−6.3	−7.9	−10.0	−10.8	−9.7	−8.6	−7.9	−6.6	−5.1	−4.4	−4.0	−4.6
	Q_{clim} (%)	−24.7	−26.4	−27.0	−27.5	−27.9	−24.6	−24.0	−22.7	−26.2	−28.1	−25.5	−24.8
	Q_{net} (%)	−23.8	−25.5	−26.1	−26.6	−27.0	−23.7	−23.1	−21.8	−25.4	−27.3	−24.7	−23.9
	Q_{lai} (%)	3.6	3.4	3.3	3.1	3.2	3.5	3.6	3.6	3.0	2.8	3.2	3.3
9	LAI total (%)	−12.5	−13.2	−15.2	−14.7	−13.4	−10.5	−9.7	−9.2	−8.0	−7.7	−7.8	−9.9
	Q_{clim} (%)	−16.1	−12.2	−12.3	−18.7	−19.3	−25.5	−31.5	−33.2	−38.4	−44.0	−36.1	−28.8
	Q_{net} (%)	−13.5	−9.6	−9.7	−16.3	−16.9	−22.6	−28.0	−30.2	−35.8	−42.2	−34.1	−26.7
	Q_{lai} (%)	16.2	21.8	21.1	12.9	12.3	11.6	10.9	9.1	6.8	4.2	5.7	7.3
10	LAI total (%)	−10.3	−11.6	−14.9	−13.8	−12.3	−10.2	−9.4	−8.8	−7.0	−6.4	−6.2	−7.2
	Q_{clim} (%)	−31.6	−23.0	−16.6	−16.6	−19.3	−19.7	−25.5	−30.9	−40.8	−46.2	−40.6	−37.5
	Q_{net} (%)	−29.3	−20.6	−14.2	−14.3	−16.9	−17.9	−23.5	−28.5	−38.4	−44.0	−38.3	−35.4
	Q_{lai} (%)	7.4	10.5	14.4	13.5	12.6	9.2	7.9	7.9	6.0	5.0	5.6	5.6
11	LAI total (%)	−19.1	−18.3	−19.2	−17.5	−18.8	−13.9	−12.9	−13.9	−12.2	−13.0	−10.7	−15.0
	Q_{clim} (%)	12.1	13.0	3.3	−12.4	−12.0	−8.2	−20.1	−35.0	−52.1	−63.2	−53.3	−46.0
	Q_{net} (%)	12.5	13.3	3.6	−12.2	−11.9	−7.1	−13.7	−26.2	−43.7	−57.8	−48.4	−41.5
	Q_{lai} (%)	−3.2	−2.2	−7.9	1.5	0.7	13.1	31.7	25.1	16.2	8.5	9.2	10.0
12	LAI total (%)	−17.7	−17.0	−19.1	−17.2	−19.4	−14.0	−12.4	−13.6	−11.3	−12.1	−9.2	−13.1
	Q_{clim} (%)	−21.1	−19.3	−18.8	−18.8	−17.9	−16.6	−22.0	−35.3	−45.0	−50.3	−34.6	−31.6
	Q_{net} (%)	−14.4	−12.3	−11.9	−12.7	−12.9	−11.8	−16.5	−27.8	−37.9	−43.8	−29.3	−25.6
	Q_{lai} (%)	31.6	36.5	36.8	32.3	28.3	28.9	25.3	21.3	15.7	12.8	15.3	19.1
13	LAI total (%)	−16.9	−16.8	−19.5	−17.8	−19.5	−14.7	−13.6	−14.5	−12.2	−12.7	−10.1	−13.5
	Q_{clim} (%)	10.4	10.1	5.7	−11.0	−11.3	−10.5	−18.8	−29.0	−43.4	−52.2	−34.2	−17.7
	Q_{net} (%)	11.0	10.7	6.6	−10.7	−10.9	−8.1	−14.7	−24.3	−38.2	−47.7	−32.3	−15.5
	Q_{lai} (%)	−5.6	−6.4	−16.8	2.6	3.8	23.0	21.6	16.3	12.0	8.4	5.5	12.3

* P (%) is the change in mean annual precipitation in percentage, T (°C) is the change in mean annual temperature in °C, Q_{clim} indicates the climate effect on runoff, Q_{net} is the net effect of climate and LAI on runoff and Q_{lai} is proportion of the climate effect (Q_{clim}) that is offset by the LAI effect.

HESSD
11, 10593–10633, 2014

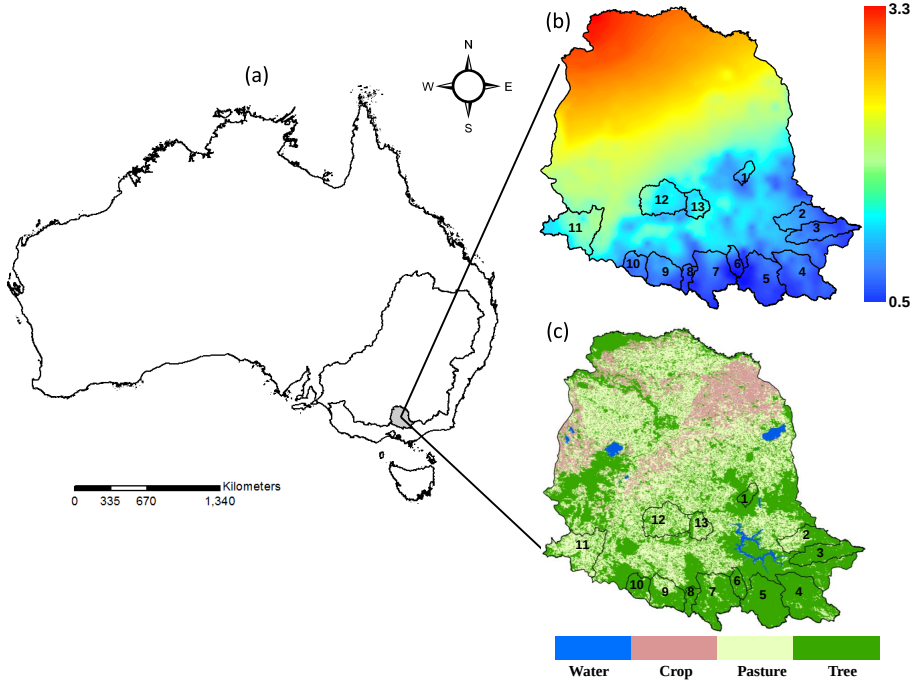

Figure 1. Location map of the study area **(a)**, dryness index (mean annual reference evapotranspiration divided by mean annual precipitation) **(b)** and land cover type **(c)**.

HESSD
11, 10593–10633, 2014

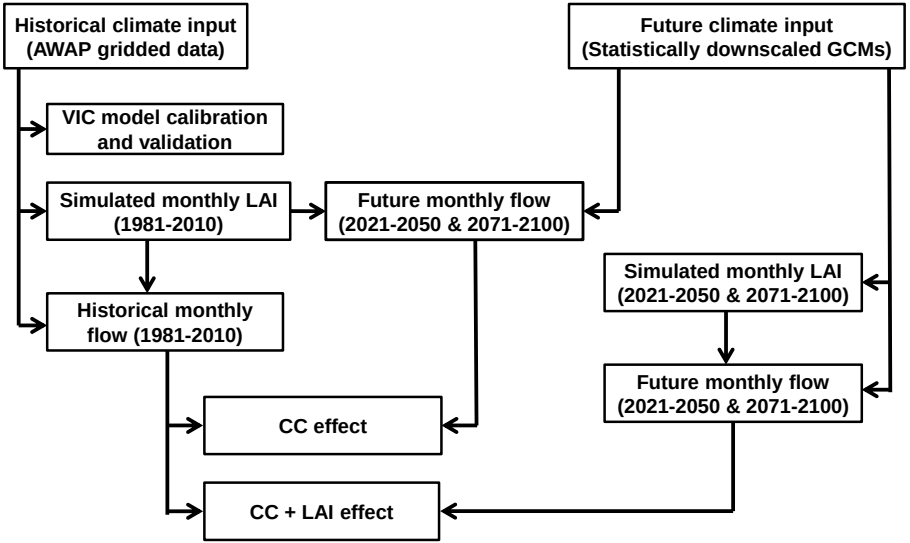

Figure 2. Flowchart showing procedure of the modelling experiments. CC effect indicates the climate change effect of precipitation and temperature, CC + LAI effect indicates the climate change effect of precipitation, temperature and leaf area index.

HESSD
11, 10593–10633, 2014

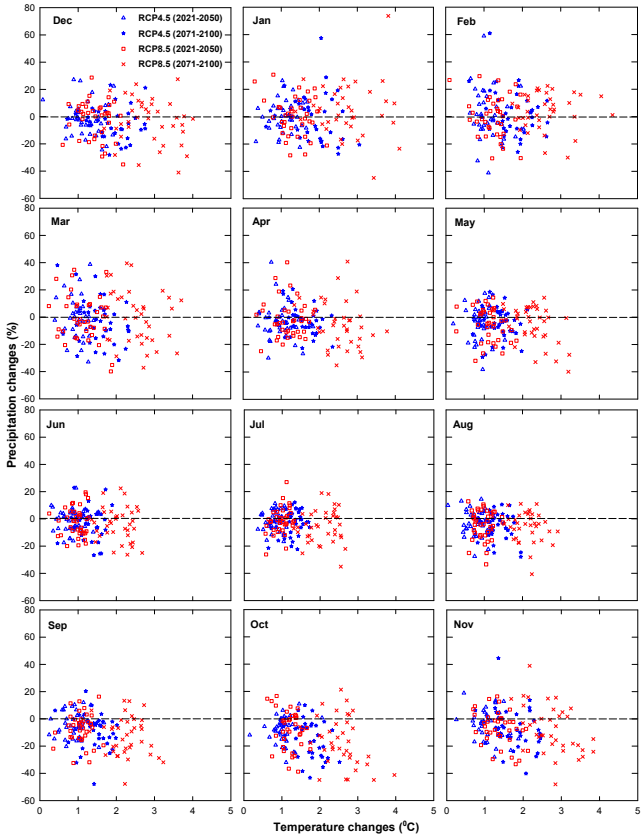

Figure 3. Percentage changes in the mean monthly precipitation plotted against changes in mean monthly temperatures in the Goulburn–Broken catchment for the future periods 2021–2050 and 2071–2100 given by each of the 38 CMIP5 runs of climate projections from the historical (1981–2010) mean monthly precipitation and temperatures.

HESSD
11, 10593–10633, 2014

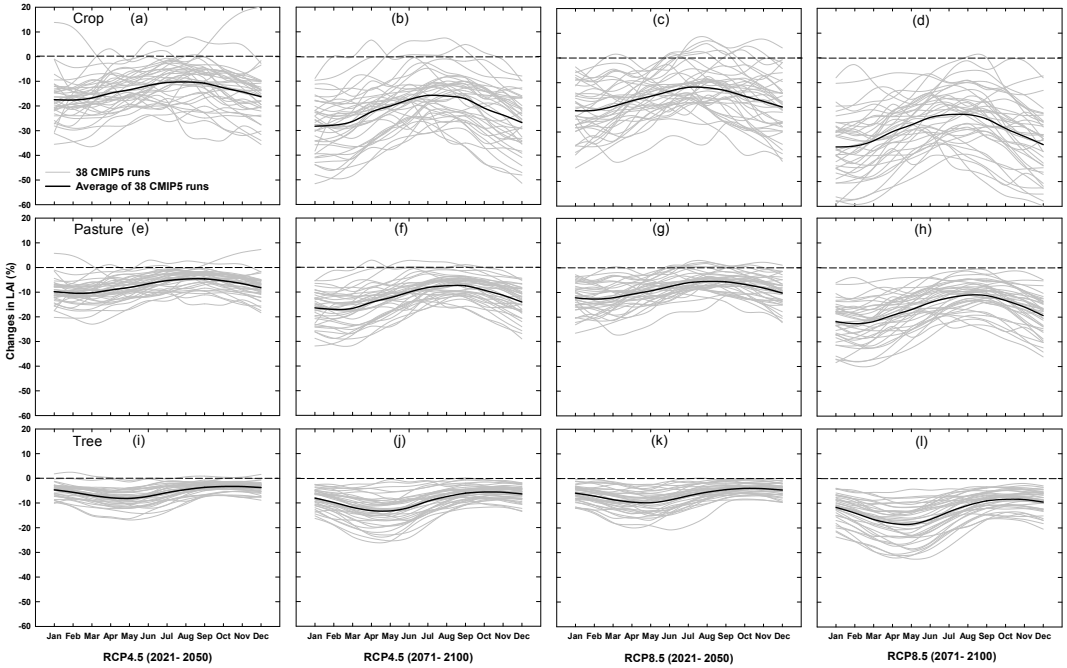

Figure 4. Changes of mean monthly LAI derived from 38 CMIP5 runs of climate projections under RCP4.5 and RCP8.5 scenarios from the historical (1981–2010) for crop **(a–d)**; pasture **(e–h)** and tree **(i–l)** in the Goulburn–Broken catchment.

HESSD
11, 10593–10633, 2014

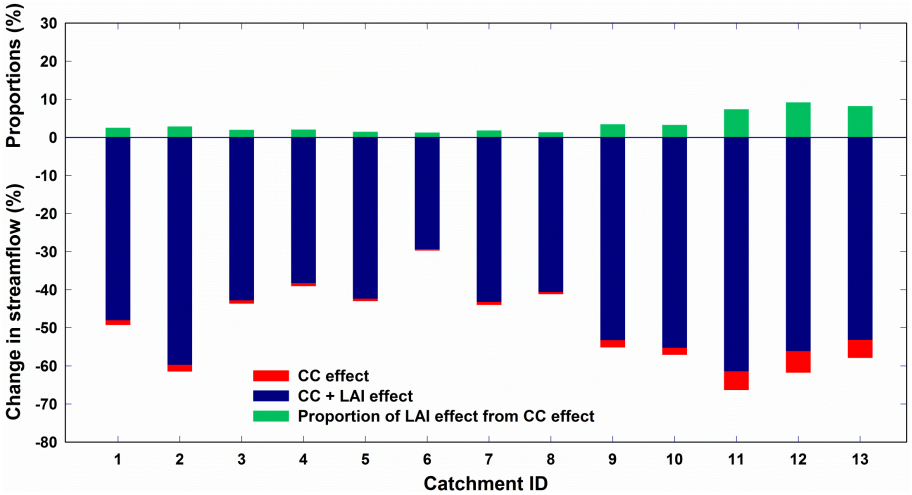

Figure 5. Impacts on catchment mean annual streamflow of the "Millennium drought" 1997–2009 relative to the period 1983–1995. CC effect indicates precipitation and temperature effect; CC + LAI effect indicates precipitation, temperature and LAI effect (all bars started from the *x* axis).

HESSD
11, 10593–10633, 2014

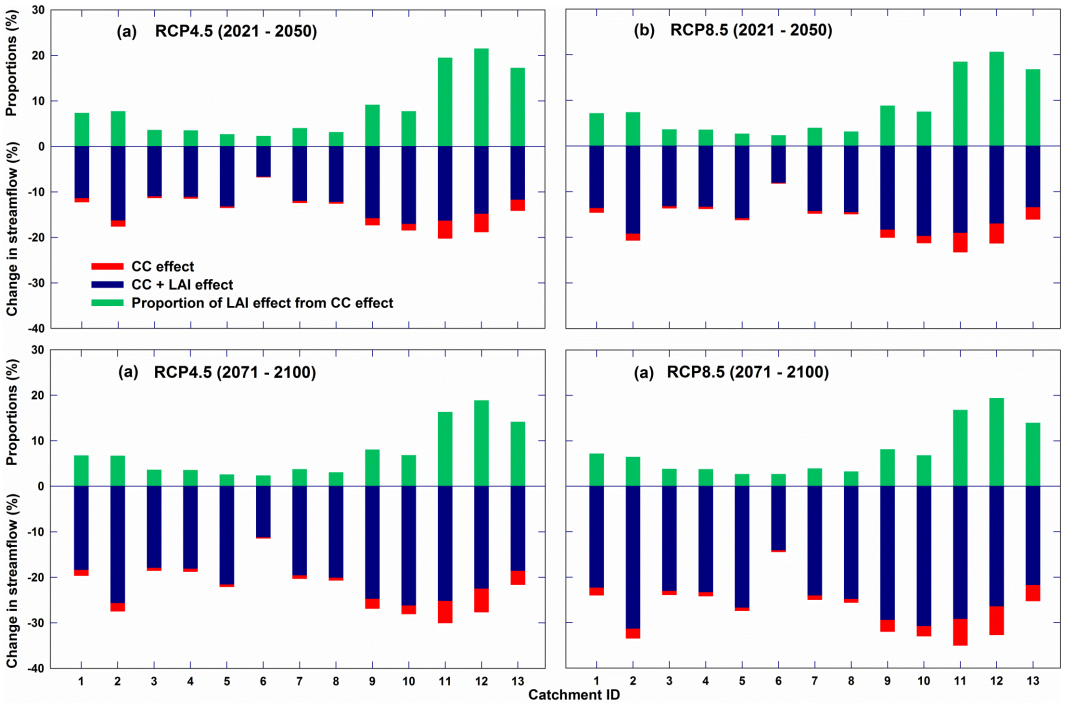

Figure 6. Impact on catchment mean annual streamflow of projected climate change for the future periods 2021–2050 and 2071–2100 under RCP4.5 and RCP8.5. CC effect indicates precipitation and temperature effect; CC + LAI effect indicates precipitation, temperature and LAI effect (all bars started from the *x* axis).

HESSD
11, 10593–10633, 2014

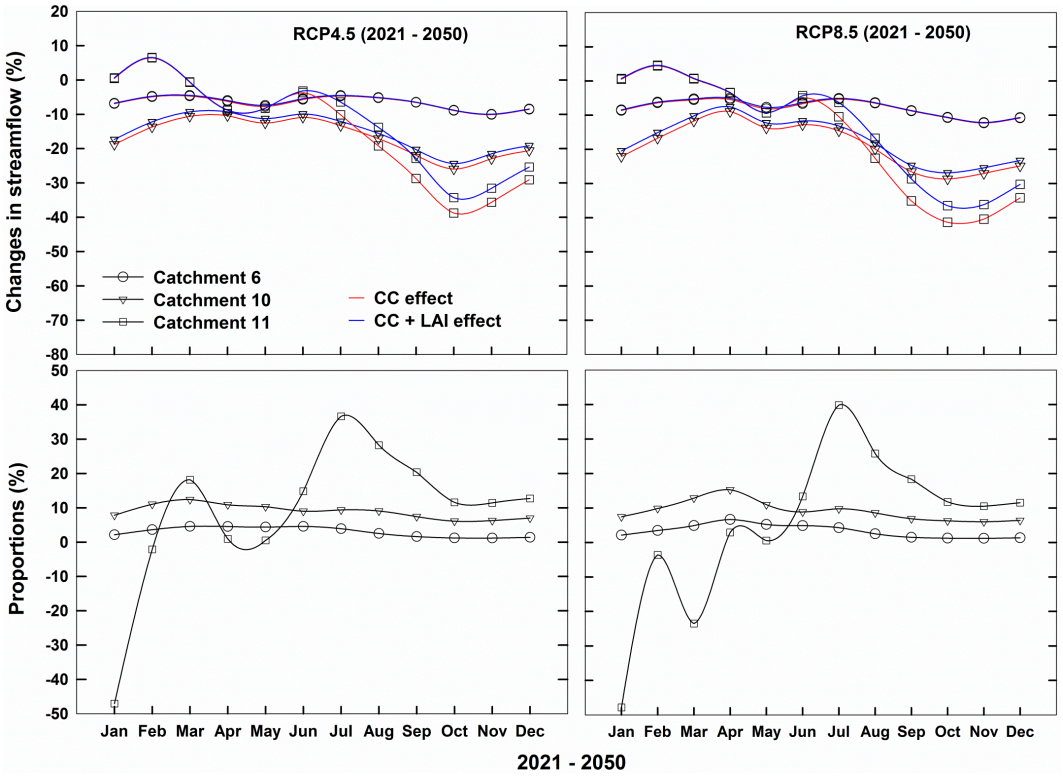

Figure 7. Impact on mean monthly streamflow from catchments 6, 10 and 11 of projected climate change for future periods 2021–2050 under RCP4.5 and RCP8.5. CC effect indicates precipitation and temperature effect; CC + LAI effect indicates precipitation, temperature and LAI effect.

HESSD
11, 10593–10633, 2014

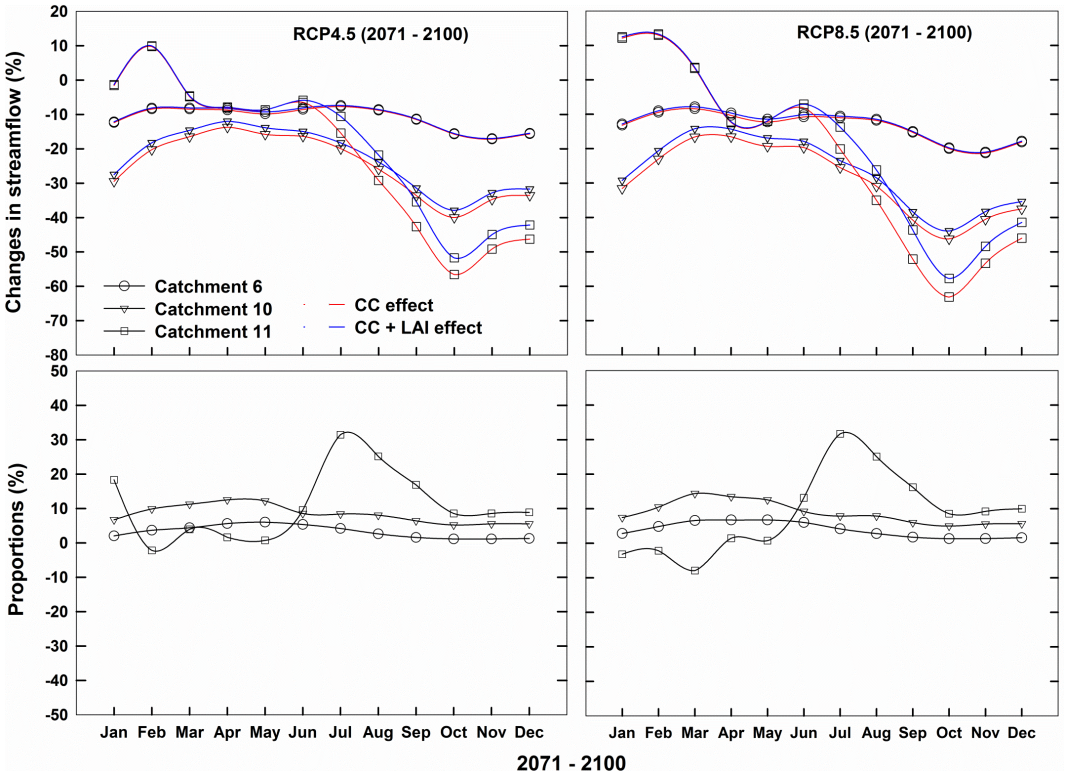

Figure 8. Impact on mean monthly streamflow from catchments 6, 10 and 11 of projected climate change for future periods 2071–2100 under RCP4.5 and RCP8.5. CC effect indicates precipitation and temperature effect; CC + LAI effect indicates precipitation, temperature and LAI effect.

HESSD
11, 10593–10633, 2014

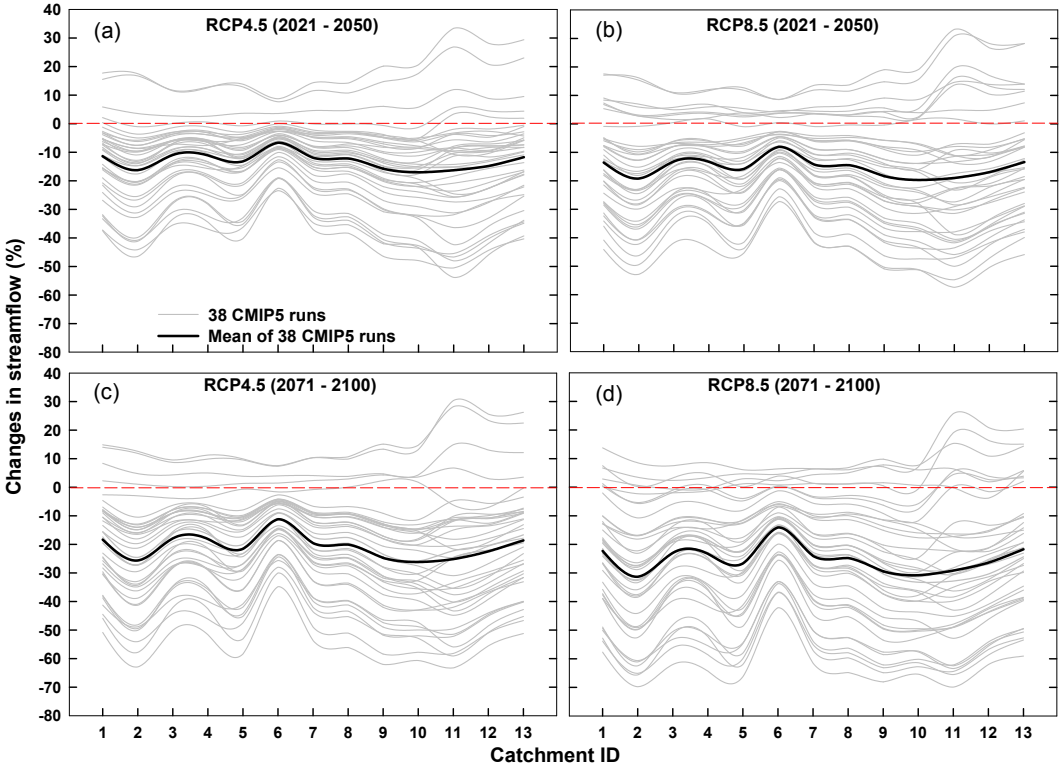

Figure 9. Percentage changes in mean annual runoff driven by climate forcing from each of the 38 CMIP5 runs as compared to the historical (1981–2010) period.

HESSD
11, 10593–10633, 2014

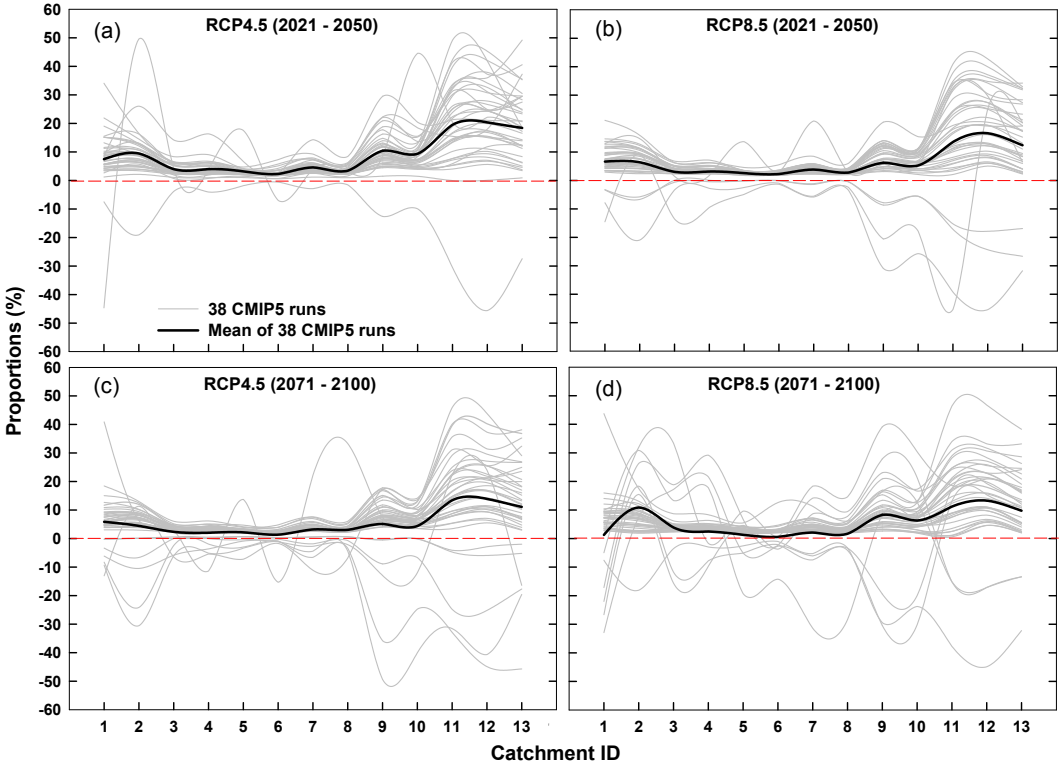

Figure 10. Percentage contribution of the LAI effect of climate change from the primary input effect in the mean annual runoff driven by climate forcing from each of the 38 CMIP5 runs as compared to the historical (1981–2010) period.

HESSD
11, 10593–10633, 2014